Environmental Pollution 265 (2020) 114795

Contents lists available at ScienceDirect

Environmental Pollution

journal homepage: www.elsevier.com/locate/envpol

An integrated assessment of land-use change impact, seasonal variation of pollution indices and human health risk of selected toxic elements in sediments of River Atuwara, Nigeria☆

PraiseGod Chidozie Emenike [a, b, *], Imokhai Theophilus Tenebe [c], Jordan Brizi Neris [d], David Olugbenga Omole [a], Olaniyi Afolayan [a], Chukwueloka Udechukwu Okeke [a], Ikechukwu Kingsley Emenike [e]

[a] Department of Civil Engineering, Covenant University, Ota, Ogun State, Nigeria
[b] Cranfield Water Science Institute, School of Water, Energy and Environment, Cranfield University, MK43 0AL, Bedford, United Kingdom
[c] Ingram School of Engineering, Texas State University, San Marcos, TX, USA
[d] Department of Chemistry, Federal University of São Carlos, Highway Washington Luis Km 235, CEP 13565-905, São Carlos, São Paulo, Brazil
[e] Department of Microbiology, Federal University of Agriculture Abeokuta, Ota, Ogun State, Nigeria

ARTICLE INFO

Article history:
Received 6 February 2020
Received in revised form
1 May 2020
Accepted 9 May 2020
Available online 14 May 2020

Keywords:
River atuwara
Sediment quality
Pollution
Compositional data analysis
Health risk assessment
Ecological risk

ABSTRACT

River sediments contain environmental fingerprints that provide useful ecological information. However, the geochemistry of River Atuwara sediments has received less attention over the years. One hundred and twenty-six sediments from 21 locations were collected over a two-season period from River Atuwara, and a detailed investigation of the land use and land cover (LULC) change between 1990 and 2019, analysis of selected toxic and potentially toxic metal(oid)s (TPTM) (Cu, As, Cd, Pb, Ni, Cr, Zn, Fe, Co and Al) using ICP-OES, pollution index assessment, potential source identification (using center log-transformation approach), potential ecological, and human health risk assessment were conducted. The results of the LULC change revealed that the built-up area increased by 95.58 km^2, at an average rate of 3.186 km^2/year over the past 30 years. The mean concentration of metal(oid)s increased in the order of Cd < As < Cr < Pb < Co < Ni < Cu < Zn < Fe < Al, and Cd < As < Cr < Co < Pb < Ni < Cu < Zn < Fe < Al during the dry and wet seasons, respectively. Meanwhile, the statistical analysis of the data spectrum inferred possible contamination from lithological and anthropogenic sources. According to the pollution load index, 90.48% of the sediment samples are polluted by the metal(oid)s. Potential ecological risk assessment identified Ni, As, and Cd as problematic to the ecological community of River Atuwara. Regarding the metal-specific hazard quotient via ingestion route, the risks are in order of Co ≫ As ≫ Pb > Cr > Cd > Al > Ni > Cu > Zn > Fe for both seasons and the carcinogenic risk for children via ingestion route presented a value higher than the safe limits for As, Cd, Cr, and Ni during both seasons. This outcome highlights the need for prompt action towards the restoration of environmental quality for communities surrounding River Atuwara.

© 2020 Elsevier Ltd. All rights reserved.

1. Introduction

The growth of many developing nations hinges on industrialization, extensive agriculture, port-related activities and extractive processes (Kozul-Wright and Fortunato, 2019; Oyeleran-Oyeyanka, 2015; Rodrik, 2016; UNIDO, 2018). However, most of the chemical compounds released and waste generated from these processes depreciate and degrade the quality of inland streams and rivers (Caballero-Gallardo et al., 2020). Recent reports have indicated that residential habitation, tourist, industrial, and commercial zones

☆ This paper has been recommended for acceptance by Klaus Kümmerer.

* Corresponding author. Department of Civil Engineering, Covenant University, Ota, Ogun State, Nigeria.
E-mail addresses: praisegod.emenike@covenantuniversity.edu.ng, praisegod.emenike@cranfield.ac.uk (P.C. Emenike), itt1@txstate.edu (I.T. Tenebe), jordanbrizi@gmail.com (J.B. Neris), david.omole@covenantuniversity.edu.ng (D.O. Omole), olaniyi.afolayan@covenantuniversity.edu.ng (O. Afolayan), chukwueloka.okeke@covenantuniversity.edu.ng (C.U. Okeke), kingsley.emenike.ike@gmail.com (I.K. Emenike).

https://doi.org/10.1016/j.envpol.2020.114795
0269-7491/© 2020 Elsevier Ltd. All rights reserved.

exert excessive pressure on nearby rivers through the discharge of vast amounts of pollutants (Fernandez-Maestre et al., 2018; Gao et al., 2018). These chemicals or waste effluents released in the form of metal(oid)s affect the quality of surface water and groundwater systems.

The process of industrialization and urbanization is advantageous, especially in the aspect of modelling demographic characteristics, but the unsystematic, unplanned, uncontrolled, and rapid transformation of physical landscape may impact negatively on several environmental components, particularly on water and land (Patra et al., 2018). In light of this, several researchers have highlighted the need to understand urbanization drifts induced by land use and land cover (LULC) change because urban transformation is at the expense of global energy which may result in environmental deterioration and degradation of the ecological community through air, soil and water pollution (Battista and de Lieto Vollaro, 2017).

The issue of metal(oid)s in the environment has turned out to be a global menace because of its bioaccumulation properties, toxicity, and persistence. Considering the rate of industrial boom in developing countries, the presence of these chemical pollutants in river systems is paramount, and the outcome is bound to impact negatively on biotic community and aquatic ecosystem (Keshavarzi et al., 2018; Ouyang et al., 2018; Sun et al., 2019). The moment metal(oid)s blend with organic species, it causes eco-interference, detrimental effect on aquatic life, and negative influence on human health via accumulation in the food chain or through different exposure pathways (He et al., 2019; Keshavarzi et al., 2018). The distribution of metal(oid)s in sediments, biogeochemical interactions and hydrodynamic conditions influence the biotic community, providing insight on their adsorption process, transport and dispersion mechanism, and formation of organic matter-contaminant complexes in an aquatic environment (Akhbarizadeh et al., 2017; Duodu et al., 2016; Pandey and Singh, 2017).

Sediments are now being considered as a derivative source and sink for metal(oid) pollutants, and over time, serves as a biomarker for investigating the impact of anthropogenic pollution up to the present day (De Vivo et al., 2017; Mao et al., 2020). Thus, analysing river sediment for hazardous metal(oid) pollutants evaluates the burden posed by anthropogenic or human activities on an aquatic environment. Interestingly, such analysis is significant because the toxic weight of these pollutants on the biota is often embedded in the environmental matrix of sediments (Celis-Hernandez et al., 2018; Kusin et al., 2018; Maanan et al., 2015). Based on these reasons, the knowledge derived from chemical distribution in sediments from riparian zones and rivers provides a holistic overview of the associated risk posed on the ecosystem or humans through exposure (Li et al., 2019).

Riparian zones acting as aquatic-terrestrial links play a significant role in the environment by maintaining the balance between riverbank stability, water quality and aquatic biodiversity (Liu et al., 2016). Globally, riparian areas are considered as natural buffers that filter pollutants between upland regions and open waters, as well as reducing erosion at the stream bank (Ramião et al., 2020). Some investigators have reported other essential ecosystem services that riparian zones provide which include flow regulation, flood attenuation and nutrient filtration (DeVore et al., 2016; Liu et al., 2019; Ramião et al., 2020; Xiang et al., 2016). Studies in Europe and other parts of the world have further revealed that riparian zones act as an effective harbour for metal(oid)s arriving via river flooding or migration from the upland region through the mechanism of adsorption and sedimentation, and their study has improved water quality framework since they are considered as fundamental elements that describe the hydromorphological conditions of the environment (Del Tánago and De Jalón, 2006; Pavlović et al., 2016). Considering the increasing rate of urbanization and intensified land use, riparian areas are undergoing drastic and accelerated transformations, in which anthropogenic activities have degraded their systems in recent times. Therefore, the rehabilitation of degraded riparian soils and river sediments after exceeding safety limits involves an in-depth understanding of the ecological and hydrological function in order to administer the best management strategy.

Over the years, Ado-Odo Ota in Ogun State, Nigeria has experienced urban transformation because of its industrial endowments (Ogbiye, 2011; Omole, 2011). Due to the accelerated urbanization rate and industrial development, human activities within the region increases continually. River Atuwara is a popular river that navigates through Ado-Odo Ota, providing economic value to its surrounding riparian communities (Emenike et al., 2020a, 2020b). These riparian communities located close to River Atuwara have a combined population of 500,000 individuals, and studies have shown that living within river path may pose a significant threat to river health since anthropogenic/human activities affect urban habitat considerably (Alqurashi and Kumar, 2019; Hua and Ping, 2018; McGrane, 2016). Hence, the variation in LULC change within the study region requires monitoring. Previous studies have indicated that industrial activities within the region practice indiscriminate disposal of waste effluents into River Atuwara (Ogbiye, 2011). This chaotic action deposits potentially hazardous metal(oid) pollutants which eventually get attracted to fine-grained particles and settle as sediments. Hence, the rationale of the current investigation lies on (1) understanding the dynamics of urbanization of the study region through LULC change (2) estimating the concentration of accumulated metal(oid)s (Cu, As, Cd, Pb, Ni, Cr, Zn, Fe, Co and Al) in the sediments of River Atuwara and establishing their inter-relationship with potential anthropogenic origin using compositional data analysis (3) using sediment quality indicators such as enrichment factor, geo-accumulation index, pollution index, pollution load index, potential ecological risk index, toxic risk index, and modified hazard quotient to assess the degree of pollution, as well as the ecological rating of the river sediments (4) assessing the potential human health risk posed by exposure to sediments via ingestion and dermal pathways. It is noteworthy to mention that this study might be the first report on sediment quality of the riparian areas of River Atuwara. Therefore, the information contained in the current study is expected to help environmental managers and key stakeholders to develop a sustainable urban development framework, comprehensive policies for urban management and planning, and workable mechanism to protect ecological quality and aquatic biota.

2. Materials and methods

2.1. Description of the study area

River Atuwara (Fig. S1) is a tributary of River Ogun and belongs to the Ogun-Oshun River catchment in Ado-Odo Ota in Ogun State, Nigeria (Latitude: 6°40′57.84″ and Longitude: 3°8′52.03″). River Atuwara emanates from Igbo-Elerin region and flows towards Ifo community. River Atuwara is regarded as an environmental treasure to surrounding communities harbouring up to 500, 000 residents that depend on it for their domestic and economic purpose (National Population Commission, 2010). The river passes through several communities located in the west of the Atlantic Ocean and connects to other nearby rivers up to 65 km away from its source. The communities that benefit from River Atuwara include Agbara, Owode-Egba, Balogun, Iju, Odo-itele, Odo-Ogbe, Igboloye, and Adefarasin. River Atuwara is connected to a swampland that irrigates more than half of the River Atuwara basin, and towards its

right side is River Mosafejo, Afara-Meje and River Balogun. Due to the tidal variability around the river, most of the unplanned drainages are now waterlogged and transformed into wetlands. Around Ado-Odo Ota lies both small-scale businesses and manufacturing firms that practice unapproved disposal of partially treated or untreated effluents into River Atuwara. Ado-Odo Ota accommodates manufacturing firms and small enterprise that engage in plastic and rubber production, fabrication from steel, iron and other metals, wood and wood products, pharmaceuticals, distilleries, soap production, food and beverages, abattoir, and paint spraying. Data used for this study were obtained between April and October (wet season), and November to March (dry season) of 2018.

2.2. Land use and land cover (LULC) classification

Analysis of land use/land cover (LULC) change was actualised by extrapolating multi-temporal satellite imageries from Landsat to comprehend spatial and temporal variations of the study region. A geo-referencing technique involving the use of ground control points was adopted, whereas WGS1984 was selected as the projected coordinate. The LULC apportionment was done based on the identification and definition of training sites with the help of ground surveillance points, and visual clarification of chronographic maps and Google Earth Imageries. Complimentary scenes of the Landsat maps were extracted from the United States Geological Survey (USGS), earth explorer website (https://earthexplorer.usgs.gov/).

To designate LULC classes and characterise the signature files, unsupervised ordering procedure related to the K-means clustering algorithm was utilised. Meanwhile, the unsupervised categorisation served as a preparatory framework for additional classification. Predominant classes were assembled to consolidate with identical value following the center class (Bhattacharjee et al., 2019); thereafter, the classification was actualised by means of iteration until the best clustering outcome was achieved. It is noteworthy to mention that the image characterisation method is considered the preferable and most widely used technique because it contains high spectral information and maintains a high level of accuracy (Biswas and Melesse, 2016; Shawul and Chakma, 2019). The generalisation of categorized LULC maps and post-classification smoothing were initiated in ArcGIS, and the clustering expression is given as:

$$j_j = \sum_{x \in s_j(l)} \| x - z_j(l+1) \|^2 \tag{1}$$

And

$$z_j(l+1) = \frac{1}{N_j} \sum_{x \in s(l)} x \tag{2}$$

where j_j represents the clustering conditions of error sum of squares, x is the vector signifying the nth data point, z_j is the geometric centroid, N_j presents the number of samples contained in S_j which serves as the cluster class j, and. $j = 1, 2, 3, 4.....k$

The areal range of categorized LULC maps for the specified periods (1990–2019) was estimated in square kilometer (km^2), and the variation was calculated amid each period. The actual difference in LULC classification was obtained by taking into account the Normalized Difference Built-up Index (NDBI), which examines the region masked with impervious surface (concrete and asphalt). According to Zha et al. (2003), the Normalized Difference Built-up Index (NDBI) formula is given as:

$$NDBI = \frac{MIR - NIR}{MIR + NIR} \tag{3}$$

Where NIR is regarded as the near-infrared band (band no. 4 – TM, ETM+ and LISS III) and MIR is the middle infrared band (band no. 5 – TM, ETM+ and LISS III). The values gotten from the expression above varies between −1 and +1. NDBI values between 0.1 and below are relatable to non-urban features, whereas high NDBI values correspond to areas covered by impervious surfaces (Patra et al., 2018).

2.3. Sample collection

Field investigation and sediment extraction were conducted in 2018. In order to capture the chemical variations in the river sediments, we compared the sediment samples collected during the dry season (July) with that of the wet season (November). Sampling points were distributed, taking into account area representation and road accessibility. Retrieval of sediment samples was achieved with a sediment sampling tube (LaMotte EP Model 1055). After each sample collection, the sampling tube was thoroughly cleaned to avoid cross-contamination and interference. A total of 126 surface sediment samples (63 samples in the wet season and 63 samples during the dry season) were retrieved from 21 locations (Fig. S1) at 0–3 cm depth (IAEA, 2003), and non-decomposed debris (roots, animal residue and stones) was removed, after which the samples were stored in Ziploc bags. Before metal analysis, the samples were air-dried for ten days, vegetative materials removed, and, sieving was done to obtain a homogeneous mass. After that, 0.5g of the previously sieved sample was digested using HF (1 mL–40%)/HNO_3 (3 mL–65%)/H_2O_2 (1 mL–30%) solution, sealed in Teflon vessels, and transferred into a microwave system. The total concentration of trace elements (Cu, As, Cd, Pb, Ni, Cr, Zn, Fe, Co and Al) in the samples were analysed by ICP-OES (PerkinElmer DV Optima 5X00).

2.4. Quality assurance and quality control

To maintain analytical integrity, a triplicate analysis was carried out on the sediment samples (average value and standard deviation were documented). Certified Reference Material (GBW07366) and reagent blanks were used for equipment calibration, and the measurement of metal(oid) concentration in the blank yielded a <3% value of the calculated concentration in the sediment sample. Due to the low concentration obtained after analysing the reagent blanks, we conclude that there was no lab contamination detected. Re-calibration was done after analysing every three samples to maintain analytical precision, and the root standard error observed were <8% between all replicates, for both dry and wet season. After spiking with standards, the recovery of samples varied from 97.4% to 105.3%.

2.5. Data analysis

After measuring the concentration of metal(oid)s, descriptive statistics, constellation plot (C-Plot), and classification of pollution indices were achieved using JMP data analysis program, version 14.3.0. Multivariate statistical assessment comprising compositional data analysis, principal component/factor analysis (PC/FA), scree graph, and biplot were actualised using XLSTAT 2018 package. Land use and land cover (LULC) and spatial distribution of the metal(oid)s and pollution indices were evaluated with ArcGIS version 10.7. Finally, health risk assessment and pollution index assessment were employed to gain an in-depth understanding of

toxic metal(oid) pollution on the ecological community, as well as on human health.

2.6. Sediment quality guidelines (SQGs)

The adoption of Sediment Quality Guidelines (SQGs) by several investigators for toxicological evaluation of sediment-related metals has fostered the management of aquatic environments, protection of biota, and the implementation of environmental policies and regulations (Maanan et al., 2015; Souri et al., 2019). In the current study, consideration was given to a few of the SQGs which include; The Probable Effect level (PEL), Threshold Effect Level (TEL), Severe Effect Level (SEL), Effect Range Low (ERL), Lowest Effect Level (LEL), and the Effects Range Medium (ERM) standards. These guidelines were used to assess the potential biological impact of metal(oid)s measured in the sediment samples.

2.7. Pollution Assessment methods

2.7.1. Geo-accumulation index (Igeo)

Geo-accumulation Index (*Igeo*), developed by Muller, is a quantitative method of classifying metal(oid) contamination (Müller, 1969). It is a tool used to distinguish anthropogenic impact, and it represents the distribution of metal(oid)s in relation to the geochemical background in the sediments (Liu et al., 2017). *Igeo* is obtained using the equation below;

$$I_{geo} = \log_2\left(\frac{C_n}{1.5B_n}\right) \tag{4}$$

where C_n is the concentration of metal, B_n is the metal background value, 1.5 is a factor used to minimise the impact of background variability caused by lithological variation. The Igeo rating is graded according to seven enrichment classes; Igeo ≤ 0 (Uncontaminated), $0 \leq$ Igeo < 1 (Uncontaminated to moderately contaminated), $1 \leq$ Igeo < 2 (Moderately contaminated), $2 \leq$ Igeo < 3 (Moderately to strongly contaminated), $3 \leq$ Igeo < 4 (Strongly contaminated), $4 \leq$ Igeo < 5 (Strongly to extremely contaminated), Igeo > 5 (Extremely high contaminated).

2.7.2. Enrichment factor (EF)

This index measures possible anthropogenic influence on metal(oid) concentration in sediments. To pinpoint the impact of anthropogenic activities on the sediment, the measured concentration of metal(oid) is compared to a conservative element not influenced by weathering, e.g. Al, Fe, Ca, Sc, Ti, or Mn (Sucharovà et al., 2012). In this study, Fe was selected as the conservative metal, and the equation used to calculate the enrichment factor (EF) is given as

$$EF = \left(\frac{C_{n\ \ (Sample)}}{C_{Fe\ \ (Sample)}}\right) \Big/ \left(\frac{B_{n\ \ (background)}}{B_{Fe\ \ (background)}}\right) \tag{5}$$

where $(C_{n\ \ (Sample)}/C_{Fe\ \ (Sample)})$ is the ratio of metal concentration and Fe concentration of the sample, and $(B_{n\ \ (background)}/B_{Fe\ \ (background)})$ is the ratio of metal background concentration to Fe concentration of the background. The background samples were retrieved from the upper stretch of the River, from an unpolluted or pristine substance unaffected by anthropic events. The background samples were comparable with the investigated samples and treated in a similar way as the sediment samples (Brady et al., 2014a). To interpret the EF values, EF < 2 is considered as Deficiency to minimal mineral enrichment, EF $= 2-5$ as Moderate enrichment, EF $= 5-20$ as Significant enrichment; EF $= 20-40$ as Very high enrichment, and EF > 40 as Extremely high enrichment (Sakan et al., 2009).

2.7.3. Single pollution index (PI) and pollution load index (PLI)

Pollution Index (PI) is achieved by multiplying the concentration of the individual metal with the inverse of the background value (Hakanson, 1980). The expression is given as;

$$PI = C_n \times \frac{1}{B_n} \tag{6}$$

The Pollution load index (PLI) evaluates the degree of contamination in the sediment. Moreover, it is a simplified approach to show the extent of soil deterioration in relation to metal(oid) build-up. The PLI is the geometric evaluation of the individual PI, and its equation is given as;

$$PLI = \sqrt[n]{PI_1 \times PI_2 \times PI_3 \times \ldots PI_n} \tag{7}$$

Where n is the number of metal analysed, and the PLI rating is given as PLI > 1 (Polluted), PLI $= 1$ (Baseline levels of pollution), and PLI < 1 (Not polluted) (Seshan et al., 2010).

2.7.4. Potential ecological risk index (PERI)

Potential ecological risk index (PERI), proposed by Hakanson (1980) determines the ecological impact and potential risk of metal(oid) exposure. It is regarded as the addition of metal-specific potential risk. It illustrates ecological vulnerability towards toxic compounds and gives a comprehensive representation of the ecological risk caused by a broad spectrum of toxic metals (Douay et al., 2013). The appraisal of the total risk index (RI) of PERI is obtained using Eq. (8)

$$RI = \sum_{i=1}^{n} E_r^i = \sum_{i=1}^{n} T_r^i \times PI^i \tag{8}$$

E_r^i is the potential ecological risk factor, T_r^i is the toxic-response factor of metal(oid) given as 5, 10, 30, 5, 5, 2, and 1 for Cu, As, Cd, Pb, Ni, Cr, and Zn respectively (Hakanson, 1980; Weissmannová and Pavlovský, 2017; Zhang et al., 2014; Zhu et al., 2013). The E_r^i rating is given as; Er < 40 (Low ecological risk), $40 <$ Er ≤ 80 (Moderate ecological risk), $80 <$ Er ≤ 160 (Considerable ecological risk), $160 <$ Er ≤ 320 (High ecological risk), Er > 320 (Serious ecological risk). Furthermore, the PERI rating is given as PERI <150 (Low ecological risk), $150 <$ PERI < 300 (Moderate ecological Risk), $300 <$ PERI < 600 (High potential ecological Risk), and PERI ≥ 600 (Significantly high ecological Risk).

2.7.5. Toxic risk index (TRI)

Zhang et al. (2016) developed a new pollution index that considers the TEL and PEL values. The Toxic Risk Index (TRI) takes into account the acute toxicity of trace metals in sediments with their relative effect. TRI can be calculated by the formula below;

$$TRI_i = \sqrt{\frac{(C_i/TEL_i)^2 \big/ (C_i/PEL_i)^2}{2}} \tag{9}$$

Where C_i is the concentration of the *ith* metal and TEL and PEL are the threshold effect level and probable effect level of the *ith* metal. The TRI ratings are as follows; TRI ≤ 5 (No toxic risk), $5 <$ TRI ≤ 10 (Low toxic risk), $10 <$ TRI ≤ 15 (Moderate toxic risk), $15 <$ TRI ≤ 20 (Considerable toxic risk), and TRI > 20 (Very high toxic risk).

2.7.6. Modified hazard quotient (mHQ)

This new index evaluates sediment contamination by comparing metal contents in the sediments with effect level standards (PEL, SEL, and TEL) (MacDonald et al., 2000). The Modified Hazard Quotient (*mHQ*) is considered a significant tool because it exemplifies the extent of risk each metal(oid) poses to the biota and aquatic habitat (Benson et al., 2018). The *mHQ* ratings are as follows; $mHQ > 3.5$ (Extreme severity of contamination), $3.0 \leq mHQ < 3.5$ (Very high severity of contamination), $2.5 \leq mHQ < 3.0$ (High severity of contamination), $2.0 \leq mHQ < 2.5$ (Considerable severity of contamination), $1.5 \leq mHQ < 2.0$ (Moderate severity of contamination), $1.0 \leq mHQ < 1.5$ (Low severity of contamination), $0.5 \leq mHQ < 1.0$ (Very low severity of contamination), and $mHQ < 0.5$ (Nil to very low severity of contamination). The *mHQ* is evaluated following the mathematical expression below;

$$mHQ = \sqrt{\frac{C_i}{TEL_i} + \frac{C_i}{PEL_i} + \frac{C_i}{SEL_i}} \tag{10}$$

2.7.7. Health Risk Assessment

The adoption of the Health Risk Assessment (HRA) model to evaluate the degree of risk posed by potentially toxic metal(oid)s on humans has gained recognition over the years. The calculation for oral exposure pathway obtains the chronic daily intake (*CDI*, for noncancer) and cancer risk (*CR*) using the chemical concentration found in the sediment sample to which the population/receptors are exposed to over a particular period (US EPA, 1989). Following that, the hazard quotient (*HQ*) is derived using the ratio of *CDI* to the oral reference dose (*RfD*, chemical-specific). The *CR* is estimated by multiplying the *CDI* by the slope factor (cancer). In this study, we assessed the HRA of the metal(oid)s in the sediments considering two population category differently (Adult and Child) based on their physiological and behavioural discrepancies, and two exposure routes (ingestion and dermal) (US EPA, 2005).

Recently, the United States Environmental Protection Agency (US EPA) itemised the need to include the relative bioavailability (RBA) factor in HRA calculation to make the assessment realistic. US EPA (2012) added that the degree of uncertainty in adopting risk-based decisions at a given site could be reduced when the RBA factor is considered. Interestingly, the RBA factor modifies the chronic dose of metal(oid)s/chemicals in sediments since the bioavailability of chemical compounds in sediments tend to be lesser than the original chemical form in diet or water (ITRC, 2017). However, several factors affect the bioavailability of metal(oid)s/chemicals in soil; they include chemical structure, solubility, biodegradability, and diffusion (NRC, 2003). The equations (Eqs 11–18) used to estimate the risk assessment of metal(oid) exposure on the population (*CDI, HQ, and CR*) are listed in the Appendix section (Appendix 1). However, it is noteworthy to mention that default RBA values have been developed by the US EPA to support HRA calculations. The default values can be replaced when an accurate site-specific RBA value is obtained. In line with this, the default RBA values were used in the present work.

2.8. Compositional data analysis (CDA)

Geochemical parameters related to sediments, soil, and water have been regarded as compositional data because they carry useful information embedded in elemental ratios (Pawlowsky-Glahn and Buccianti, 2011). In practice, the network of compositional data has been administered to explore the origin of toxic elements, visualise the distribution of elements, and identify the impact of anthropogenic and geodetic actions in the environment (Petrik et al., 2018b). Compositional data consist of vectors grouped into D-dimensional simplex space containing positive real components (Aitchison, 1999, 1982). Before applying the multivariate statistical technique to geochemical data, adequate data treatment should be employed to retain the compositional data attributes and inter-parameter relationship. However, some log-ratio transformations have been identified in the literature to analyse and treat data structure in Euclidean space where multivariate analysis technique can be deployed (Egozcue et al., 2003). The centered log-ratio (Clr) and additive log-ratio (Alr) transformation, introduced by Aitchison (1982), and subsequently, the isometric log-ratio (Ilr) transformation by Egozcue et al. (2003) has been put forward to reveal the complementary structures of variables extracted from an investigated terrain. In addition, the underlying factors governing the data variability can be explained better when a log-ratio transformation is employed (Wang et al., 2019).

In the current investigation, we employed the Clr–transformation because of the following benefits (i) the Aitchison distance relatable compositions are equivalent to the Euclidean distance that exists between the vector components of Clr coefficients (ii) the power of compositions and perturbation is converted to ordinary addition and product functions with the help of Clr coefficients. Moreover, one shortfall of the Clr–transformation is that it possesses a singular covariance matrix. Despite this disadvantage, the ability to freely analyse the relationship between chemical variables is the main reason this study chose to adopt the Clr technique for our statistical evaluations.

In real-time, these attributes exemplify the importance of the Clr coefficients. Meanwhile, the Clr-transformation is obtained using the expression below:

$$\begin{aligned} Clr\left(x\right) &= \left(\ln \frac{x_1}{\sqrt[D]{x_1 \cdot x_2 \cdot x_3 \cdot \cdots \cdot x_D}}\right) \\ g\left(x\right) &= \sqrt[D]{x_1 \cdot x_2 \cdot x_3 \cdot \cdots \cdot x_D} \\ \therefore Clr\left(x\right) &= \left(\ln \frac{x_i}{g(x)}\right) \\ &\text{where } i = 1, \ldots\ldots, D \end{aligned} \tag{19}$$

where $g(x)$ is the geometric mean (Geo-Mean) of the data set variable and x represents the specific variable data. For this kind of analysis, each component represents the log-ratio of the centered value in which the geometric mean is the divisor. The Geo-Mean binds the transformed data, and its interpretation cannot be achieved independently (Thiombane et al., 2018). Thus, any single Clr relationship is always associated with the "total" or a group of the total component. Furthermore, the multivariate analysis conducted with the Clr-transformed data produces scores that represents the data structure in Euclidean space. The outcome is based on a data matrix of variance characterized with scores and loadings to display the inter-relationship of the dataset. The plots produced contain variables serving as vector rays drawn from the midpoint in which the length is proportional to the explained variance (also known as biplot). To interpret the plot, the loadings, distance between vertices, and directional derivatives are taken into consideration, providing a detailed relationship between the samples and rays.

The adoption of Factor Analysis (FA) by several researchers has yielded positive impact and popularity over the years in the identification of pollutants from hypothetical origin (Petrik et al., 2018a). The inclusion of varimax rotation has also improved the interpretation of results because it simplifies the transformed dataset, and minimise the number of variables with high loadings

produced by each factor through orthogonal rotation (Reimann et al., 2002). In as much as multivariate statistical assessment (MSA) allows samples with identical chemical and physical attributes to be categorized together, trend patterns that provide essential information about the controlling factors of geochemical compositions may not be identified immediately (Güler et al., 2012). Therefore, it is important to merge the results obtained from the MSA with other analysis to provide an elaborate interpretation of the data structure (Blake et al., 2016).

The Constellation Plot (C-Plot), derived from the Hierarchical Cluster Analysis (HCA) is often used to uncover subgroups classifications occurring within a defined dataset in relation to their similar characteristics. Interestingly, the HCA technique applies to log-transformed data (van den Boogaart; Tolosana-Delgado, 2013), as it provides adequate clarification of variables with similar geochemical behaviour or an approximate anthropogenic origin within the sample region (Thiombane et al., 2018).

3. Results and discussion

3.1. Spatial and temporal assessment of LULC change

Spatial trends and total area of LULC changes in the Ado-Odo Ota region for the year 1990, 2006, 2011 and 2019 are displayed in Fig. 1, and a significant change was observed in different LULC category over the years. The LULC change identified considerable sets of land expansion of which the built-up area increased by 95.58 km^2 over the past 30 years, at an average rate of 3.186 km^2/year, and at the expense of thick vegetation and light vegetation. (see Table S1 in supplementary material).

The post-classification difference explained in the present study examine three different phases spread over the years, i.e., from 1990 to 2006, 2006–2011, and 2011–2019. In 1990, the prevalent LULC type (in ascending order) was thick vegetation, light vegetation, and built-up area. The built-up area considered as urban settlement were agglomerated in the western arm or River Atuwara (see Fig. 1 (a)). In contrast, the region experienced a spread in the built-up area towards the eastern part of river Atuwara in 2006, as well as an increase in wetlands, light vegetation, and cultivated area (Fig. 1b). Further observation of the LULC data revealed a vast spread of built-up area in 2011 with significant increase in wetland and swamps (Fig. 1c). Furthermore, the LULC change of built-up area indicated a massive class in 2019, covering as wide as 42.45% of the total area. Light vegetation, cultivated land, thick vegetation, wetland/swamp and waterbody covered 16.29%, 12.91, 6.943%, 21.28% and 0.117%, respectively (Fig. 1d). From the results above, it is obvious that urbanization has impacted on vegetation loss, and such development will significantly increase human activities, industrialization and the possible introduction of anthropogenic contaminants.

3.2. Metal(oid) concentration in sediments

The descriptive information as contained in Table S2(a) (in the supplementary material) summarises the deposited toxic elements in the sediment samples of River Atuwara (RA) during the dry and wet seasons of 2018. Measured concentration (mean ± SD, mg/kg) in the dry season were: Cu (48.46 ± 17.82), As (7.156 ± 3.307), Cd (3.011 ± 1.721), Pb (22.65 ± 12.16), Ni (34.32 ± 27.63), Cr (17.78 ± 6.129), Zn (173.6 ± 77.87), Co (31.63 ± 10.57), Fe (354.4 ± 91.09), and Al (2868 + 1629). while the measured concentration (mean ± SD, mg/kg) in the wet season were: Cu (88.89 ± 32.88), As (11.83 ± 5.452), Cd (4.976 ± 3.067), Pb (41.88 ± 22.41), Ni (50.15 ± 40.45), Cr (31.45 ± 10.41), Zn (184.6 ± 76.79), Co (37.25 ± 10.59), Fe (363.6 ± 91.48), and Al (2899 + 1628). The sediment quality was assessed by benchmarking the concentration obtained with the Probable Effect level (PEL), Threshold Effect Level (TEL), Severe Effect Level (SEL), Effect Range Low (ERL), Lowest Effect Level (LEL), and the Effects Range Medium (ERM) values. From the results obtained, all samples surpassed the LEL value of Cu, whereas 90.48% of the sample fell between the ERL and ERM. The implication of this is that the biota of the sample region will be less affected by Cu compared with other metal(oid)s. In relation to Cu concentration in the sediments, it is probable that it emanated from anthropogenic source as it has been reported that the river receives effluents generated from a gin manufacturing factory (Tenebe et al., 2018). In the case of As, 52.38% of the samples oscillated between the TEL and PEL value, indicating a detrimental biological effect on the biota. Arsenic being a problematic metal(oid) occurs anthropogenically and naturally in organic and inorganic forms. Organic As compounds such as monomethylarsonic acid (MMA) and dimethlyarsonic acid (DMA) are considered less hazardous and carcinogenic, while the inorganic forms (arsenite and arsenate) are more mobile and highly toxic than the organoarsenic species (Ferguson et al., 2018). It is noteworthy to mention that high concentration of As in sediment has been reported to be associated with high organic matter, and its interaction with itself and other mineral surfaces often result in possible formation of organo-arsenic complexes. Organic matter may influence the release of As by altering the redox chemistry of As species and site surfaces. In sediment matrix, As oxidation is influenced by redox conditions, making it to exist in −1, +3 and + 5 oxidation states. As (−1) and As (+3) are predominant in reducing environment, while As (+5) occurs in oxidising environments (Gorny et al., 2015; Xu et al., 2011). Reports revealed that during redox fluctuations (from oxic to anoxic), sequestration of As occurs mainly through adsorption and/or binding onto Fe/Mn/Al oxides (Wang and Mulligan, 2006; Xu et al., 2011). Prieto et al. (2016) pointed out that at oxic to suboxic conditions, microbial activities influence As release in sediments by reducing arsenic to arsenite. In addition, the application of fertilisers is likely to increase As content in the sediment since they are present as galena and arsenopyrite (ELTurk et al., 2018). Also, within the sample region, reports have identified intensive agricultural activities involving the cultivation of local vegetable (Emenike et al., 2019a, 2019b; 2020a, 2020b). This suggests that the heightened As content could result from the use of sodium arsenite and gallium arsenide as pesticides, which in turn appear in sediments obtained from River Atuwara. Another possible reason for such enrichment could be attributed to urban activities and the accumulation of contaminants by runoff and washed down to the river (ELTurk et al., 2018). Also, we observed that wastewater effluents from surrounding industries are discharged secretly into River Atuwara. The high enrichment of As correlates with previous work obtained from the river water samples (Emenike et al., 2020a, 2020b).

Cadmium (Cd) concentration exceeded the PEL standard in 14.29% of the samples, whereas 85.71% of the samples fell between the TEL and PEL threshold (Table 1). Similarly, the results exemplify the likelihood of harmful effects caused by Cd on the biota. Several anthropogenic activities introduce Cd into the environment. Omole (2011) and Adewumi et al. (2011) identified the discharge of Abattoirs sludge and application of fertilisers as a potential source of Cd in River Atuwara. Consequently, these sources might be responsible for the high concentration of Cd in the sediments since there has been continuous disposal of abattoir sludge into River Atuwara. Lead (Pb) was observed to oscillate between the TEL and PEL range in 42.86% of the samples, indicating a potential hazard if attention is not given. It is possible that the level of Pb observed in the sediments may originate from the use of gasoline additive, pesticide, as well as chemical manure (Aboud and Nandini, 2009).

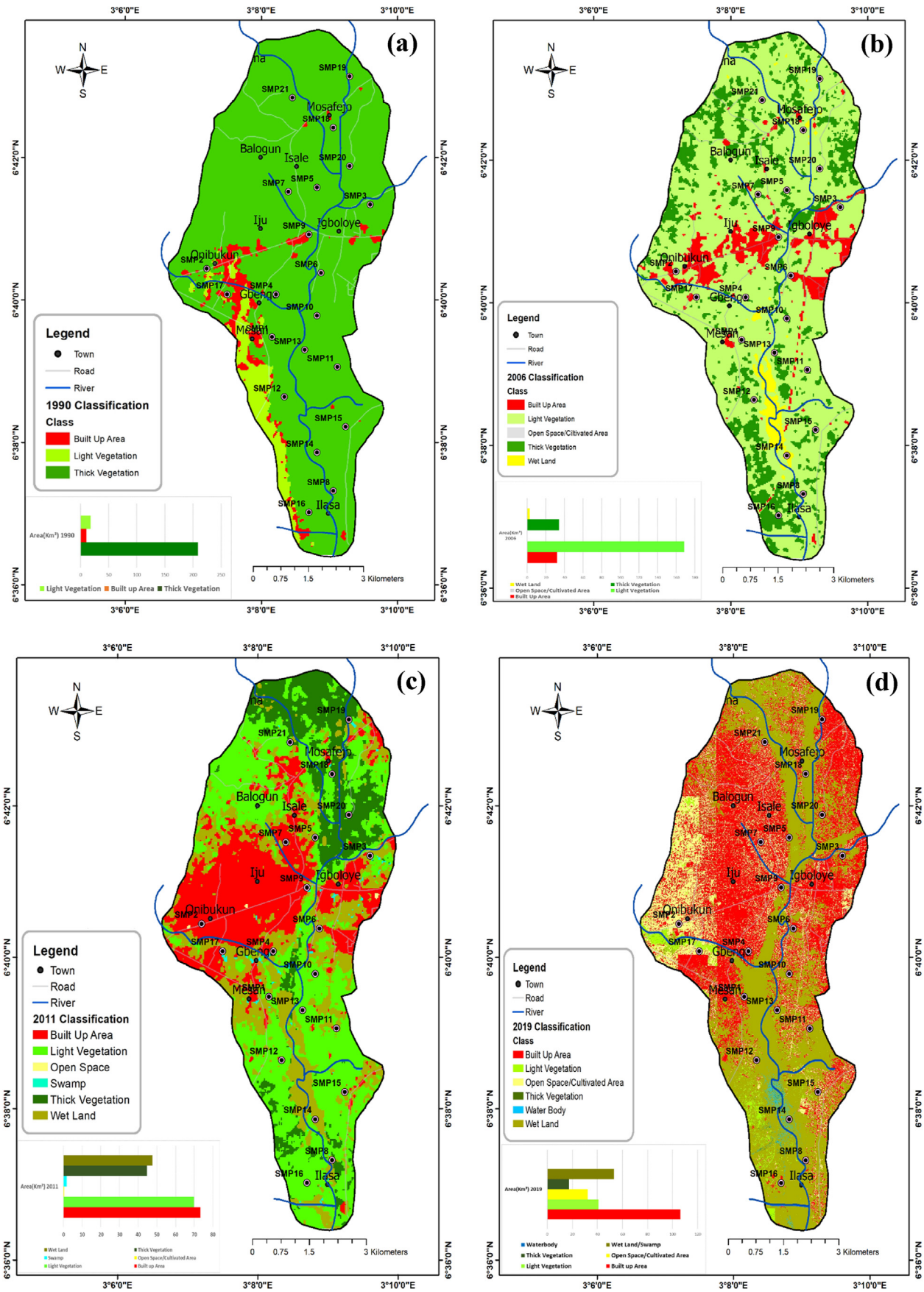

Fig. 1. Spatial representation of LULC change at the River Atuwara region (a) LULC map at year 1990 (b) LULC map at year 2006 (c) LULC map at year 2011 (d) LULC map at year 2019.

Table 1
Grouping of metal(oid)s in sediments according to sediment quality standards.

Dry Season									
	Cu	As	Cd	Pb	Ni	Cr	Zn	Co	Al
Mean	48.46	7.156	3.011	22.65	34.32	17.78	173.6	31.63	2868
Minimum	18.78	3.731	1.209	5.198	5.017	11.74	43.43	3.183	1021
Maximum	82.28	14.79	7.729	43.49	103.5	29.77	330.6	52.19	6295
% deviation from Sediment Quality Guideline									
% of Samples < ERL	9.523	66.67	None	100	33.33	100	47.62	NG	NG
% of Samples > ERM	None	None	None	None	14.29	none	None	NG	NG
% of Samples between ERL and ERM	90.48	33.33	100	None	52.38	None	52.38	NG	NG
% of Samples < LEL	None	52.38	None	61.90	23.81	80.95	33.33	NG	NG
% of Samples > LEL	100	47.62	100	38.10	76.19	19.05	66.67	NG	NG
% of Samples between TEL and PEL	100	52.38	85.71	42.86	47.62	100	52.38	NG	NG
% of Samples > PEL	None	None	14.29	None	28.57	None	9.523	NG	NG
% of Samples < SEL	100	100	100	100	85.71	100	100	NG	NG
% of Samples > SEL	None	None	None	None	14.29	None	None	NG	NG
Wet Season									
	Cu	As	Cd	Pb	Ni	Cr	Zn	Co	Al
Mean	88.89	11.83	4.976	41.88	50.15	31.45	184.6	37.25	2899
Minimum	34.16	6.208	1.802	9.749	6.301	21.14	51.97	10.93	1034
Maximum	151.4	24.46	13.39	80.31	151.3	51.54	339.1	54.48	6336
% deviation from Sediment Quality Guideline									
% of Samples < ERL	None	42.86	None	57.14	14.29	100	38.09	NG	NG
% of Samples > ERM	None	None	9.52	None	28.57	none	None	NG	NG
% of Samples between ERL and ERM	100	57.14	90.48	42.86	57.14	None	61.91	NG	NG
% of Samples < LEL	None	None	None	47.62	14.29	47.62	33.33	NG	NG
% of Samples > LEL	100	100	100	52.38	85.71	52.38	66.67	NG	NG
% of Samples between TEL and PEL	66.67	76.19	52.38	52.38	33.33	28.57	57.14	NG	NG
% of Samples > PEL	33.33	23.81	47.62	None	52.38	None	9.523	NG	NG
% of Samples < SEL	71.43	100	90.48	100	85.71	100	100	NG	NG
% of Samples > SEL	28.57	None	9.523	None	14.29	None	None	NG	NG

NG – Not Given; Concentration of metal(oid)s in mg/kg.

However, Madzin et al. (2015) reported that Pb is part of the main ore characteristics. In the sample region, dredging activities is a lucrative business amongst residents with sand extraction mainly from River Atuwara. In this regard, disruption of the main soil ore and subsequent deposition of sand at the river shore may be responsible for the presence of Pb in the sediments. Nickel (Ni) concentration in 28.57% of the samples surpassed the PEL threshold, 47.62% were between the TEL and PEL standard, and 52.38% of the samples were between the ERL and ERM limits (see Table 1). These results reveal that Ni may likely cause potential harm to sediment-dwelling organisms. High content of Ni might be derived from chemical industry waste, incineration, metallurgy, and metal plating (Palansooriya et al., 2020). However, in River Atuwara, there has been indiscriminate disposal of untreated effluent from a chemical producing factory at SMP8. Also at SMP9, there have been reports of untreated domestic waste disposal directly at the site. Concurrently, these locations mentioned are characterized by high Ni content in the sediment samples. Chromium (Cr) was observed to be high in the sediment samples wherewith 100% of the samples oscillated between the TEL and PEL standard. To add, recent studies have identified anthropogenic actions as potential contributors to Cr in coastal environments (Chen et al., 2019; Rasool et al., 2016).

The toxicity of Cr results in serious hazard because they are by-products of human-made activities such as wood preservation, tanning, and painting (Bluskov et al., 2005). From observations around River Atuwara, the activities mentioned above are popular businesses engaged by residents. Therefore, imminent pollution is paramount, causing the results to align with previous views identified within the sampling area (Omole, 2011). Zinc (Zn) concentration in 9.523% of the samples exceeded the PEL threshold, and 52.38% of the samples were within the TEL and PEL limit. High values of Zn was observed in SMP5, SMP6, SMP8, and SMP18. Further investigation and visual observation revealed that an open dumpsite is located near the sample locations mentioned above. To this end, there is a possibility of Zn leaching from the dumpsite, thereby accumulating in the sediments. Concerning Co and Al, there are no guidelines given to compare the extent of contamination in sediments.

Reports have also indicated that sediment quality differs for varying seasons (Chen et al., 2019; Zahra et al., 2014) because factors such as hydrological effects, cultural influence, lithological input and geological features may be influenced by anthropogenic activities (Zhuang et al., 2018). Several investigators have discovered that pollutants in coastal environments tend to be reduced in the wet season than in the dry season (Akindele et al., 2020). However, the works of other researchers have revealed otherwise because, at low velocity and reduced water levels, some pollutants precipitate, increasing their enrichments in coastal sediments (Bancon-Montigny et al., 2019; Caballero-Gallardo et al., 2020). In the current work, we observed high metal content in the sediment collected in the wet season than in the dry season. Al and Fe content in the sediments varied slightly, although no significant change occurred for both seasons. Meanwhile, the concentration (in percent) of other metals changed significantly during the wet season in ascending order of Pb > Cu > Cr > As > Cd > Ni > Co > Zn > Fe > Al. The results presented in this study are in accordance with the changes in land use from 1990 to 2019 which would have deteriorated the sediment quality of the river. Consequently, Ado-Odo Ota is popularly known to be an industrial hub that accommodates up to 40 industries, small and medium scale enterprise (Ogbiye, 2011). The environmental impact of the industrial cluster within the region has been left unchecked, and the reflection impacts negatively on the

environmental quality of River Atuwara. From the results, it is therefore obvious that the built-up areas of the sample region have contributed several toxic compounds to River Atuwara. Till date, no proactive measures have been administered by the government, non-governmental organizations, and polluting industries to revive the ecological quality of River Atuwara.

Moreover, pH is an important component that controls the mobility of metal(oid)s in sediments. pH values above 6.5–7.5 hinders the bioavailability and mobility of metal(oid)s through the mechanism of precipitation and adsorption (Equeenuddin et al., 2013). The negative charge at the surfaces of the clay particles are suppressed at low pH as well as the organic matter and Fe/Mn/Al oxides, resulting in increased cationic reactions wherewith cations (Fe^{3+}, H^{+} and Al^{3+}) tend to compete with metal(oid) cations for the negative sorption sites available in the sediments (Guan et al., 2018). In other words, low pH weakens the bonds existing between metal(oid)s and the sediments and impedes their absorption. In the current investigation, the pH values of the sediments ranged from 7.68 to 8.39 (mean value of 8.14) and 7.83–8.88 (mean value of 8.48) in the dry and wet season, respectively. The high values observed under different seasons showcase the relatively stable state for metal(oid)s. However, it is imperative to mention that the alkaline characteristics of the sediments may expedite the dissociation of metal species from the sediment and influence secondary pollution.

A comparison of the mean concentration of potentially toxic metals in the sediments of River Atuwara with international rivers around the world is presented in Table S2(b) (supplementary material. In general, Cr concentration in River Atuwara is lesser than the rivers highlighted in Table S2(b), Zn and Pb contents are higher in River Atuwara, Cd concentration is higher in River Atuwara, but lesser than the values obtained in Southern coast of Sfax, Tunisia (Naifar et al., 2018). Other variations can be drawn from the table.

3.3. Assessment of sediment pollution indices

3.3.1. Enrichment factor (EF)

Enrichment Factor (EF) for each metal(oid) was used to ascertain anthropogenic influence on sediment quality (Fig. 2). The values of EF during the dry season were within the following ranges: Cu 0.1712–1.764, As 1.429–12.34, Cd 0.3372–2.727, Pb 0.0856–1.394, Ni 0.1205–4.151, Cr 0.6306–2.929, Zn 0.4872–3.948, and Co 0.1571–2.106 (Fig. 2a), and during the wet season: Cu 0.3072–3.161, As 2.329–19.85, Cd 0.5069–4.724, Pb 0.1603–2.573, Ni 0.1743–6.069, Cr 1.143–5.071, Zn 0.5831–4.056, Co 0.5394–2.541 (Fig. 2b).

It has been outlined that EF values ranging between 0 and unity for any metal(oid) indicate contamination from crustal sources, whereas EF values surpassing unity signifies potential influence from anthropogenic sources (Maanan et al., 2015; Sakan et al., 2009). In this study, EF was above 1 for As (dry season, all sites), Cr (wet season, all sites), Cu, Cd, Zn and Co (dry season, ~86% of the samples). In line with this, most sediments would be subject to pollution with at least one of the studied elements. The obtained EF values were also classified in three categories of enrichment according to Sakan et al. (2009): deficient to minimal enrichment (EF = 2–5), moderate enrichment (EF = 5–20), and significant enrichment (EF = 20–40). In this sense, percentages of samples in each category of the dry season (Fig. 2a) were as follows: deficient to minimal enrichment occurred for Zn in 52.38% of the samples, Pb 100%, Cd 90.5%, Ni 85.70%, Cu 100%, Cr 85.71%, Co 85.70%, and As 4.8%; moderate enrichment: Zn 47.36%, Ni, Co, Cr, 14.28%, As 57.14%, and Cd 9.52%; significant enrichment occurred only for As in 38.09% of the samples. In the wet season (Fig. 2b), a deficient to minimal enrichment was observed for Pb and Ni in 85.71% of the samples, Cd 57.14%, Co 66.67%, Cr 33.33%, Cu 71.43%, and Zn 47.62%; moderate enrichment was observed for As 23.81%, Cd 42.86%, Co 33.33%, Cr 61.90%, Cu 28.57%, Ni 4.76%, Pb 14.28%, and Zn 52.38% and significant enrichment for As, Cr, Ni in 76.19%, 4.76%, and 9.52% of the samples, respectively (Fig. 2b).

3.3.2. Pollution index (PI) and pollution load index (PLI)

The regional transformation facilitated by LULC operation has imposed a detrimental impact on the sediments obtained from River Atuwara. In this light, there is a variation of PI observed for different metal(oid)s in the sediment samples. From Table 2, it could be seen that during the dry season, 52.38% and 47.62% of the samples were observed to be moderately polluted and unpolluted with Cu respectively. Concerning As, the investigation revealed a strong PI for all samples. Cd in the sediment samples showed a different level of pollution in which 38.1% of the samples were unpolluted, 38.1% were moderately polluted, and 23.8% of the samples were considered as strongly polluted. Pb in the sediments was categorized as unpolluted (57.14%) and strongly polluted (42.86%). Regarding Ni in the sediments of River Atuwara, moderate pollution was observed in SMP4, SMP5, and SMP6. Meanwhile, 52.38% of the samples were grouped as unpolluted and 33.33% of the sediment samples were categorized as highly polluted. Cr and Al recorded moderate pollution and low pollution respectively. However, As recorded moderate pollution in 95.24% of the samples, Zn recorded moderate pollution in 66.67%, high pollution in 23.81%, and low pollution in 9.52% of the samples. Co recorded moderate pollution in 95.24% and Al recorded low pollution in 100% of the samples.

The wet season presented a different pollution rating throughout the samples. Cu (14.29%), Cd (4.76%), Pb (33.33%), Ni (23.81%), Zn (4.76%), Co (4.76%), and Al (100%) recorded low level of pollution. Again, Cu (85.71%), Cd (52.38), Pb (66.67%), Ni (42.86%), Cr (57.14%), Zn (71.43%), and Co (95.24%) recorded moderate pollution level. Meanwhile, As (100%), Cd (42.86%), Ni (14.29%), Cr (42.86%), and Zn (23.81%) recorded strong pollution.

To examine the collective toxicity of the metal(oid)s in the sediments, the PLI was calculated. From the results, the dry season PLI rating showed that River Atuwara is polluted, having noticed that 72.19% of the sediment samples exceeded the PLI value of 1. However, 4.762% of the samples fell at the baseline pollution level, while 19.05% of the samples were considered not polluted (Fig. 2c). In general, the PLI rating categorized the pollution level into two—Polluted and Not Polluted. According to the PLI rating, 9.524% of the samples were not pollute, and 90.48% of the sediment samples were polluted by the metal(oid)s considered in the current investigation (Fig. 2d). The results buttresses the fact that the contamination level observed at the study region is a multi-metal case attributed to areas with a prolonged history of industrial events (Barandovski et al., 2015; Gaberšek and Gosar, 2018; Rinklebe et al., 2019).

3.3.3. Geoaccumulation index (Igeo)

The assessment of *Igeo* in surface sediment for the different seasons (dry and wet) are presented in Table 3. The Igeo values obtained in both seasons shows a metal to metal variation throughout the investigated site. In the dry season, the Igeo values of Pb, Ni, Cr, Zn, Co, Al, and Cu exhibited high pollution in the surface sediments. Amongst the toxic elements, As and Cd followed a different pattern of accumulation. As and Cd exhibited strong pollution in 23.81% and 9.524% of the surface sediments, respectively. The Igeo results for As and Cd also revealed that 47.62% and 33.33% of the sampled sediments were categorized under the moderate to strongly polluted class, respectively. Similarly, 23.84% and 42.86% of the sediment samples can be grouped under the

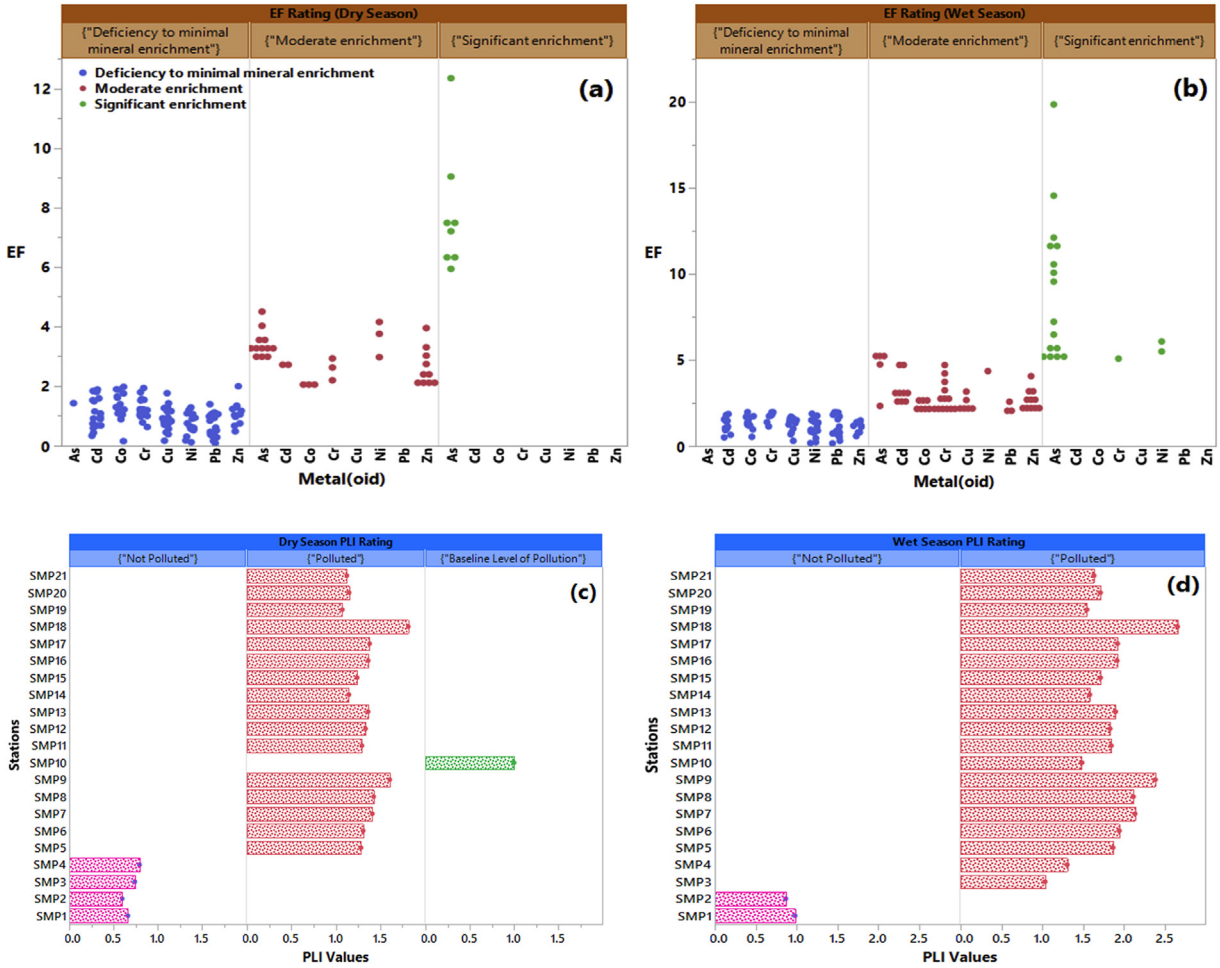

Fig. 2. Pollution Assessment indicating (a) EF Rating in the dry season (b) EF rating in the wet season (c) PLI rating in the dry season (d) PLI rating in the wet season.

Table 2
Pollution Index classification with respect to sampled location during the dry and wet season.

Pollution Index Classification	Cu	As	Cd	Pb	Ni	Cr	Zn	Co	Al
Dry Season									
PI < 1	47.62%	Nil	38.09%	57.14%	52.38%	Nil	9.524%	4.762%	All samples
1 ≤ PI ≤ 3	52.38%	Nil	38.09%	Nil	14.29%	All samples	66.67%	95.24%	Nil
PI ≥ 3	Nil	All samples	23.81%	42.86%	33.33%	Nil	23.81%	Nil	Nil
Wet Season									
PI < 1	14.29%	Nil	4.762%	33.33%	23.81%	Nil	4.762%	4.762%	All Samples
1 ≤ PI ≤ 3	85.71%	Nil	52.38%	66.67%	42.86%	57.14%	71.43%	95.24%	Nil
PI ≥ 3	Nil	All Samples	42.86%	Nil	14.29%	42.86%	23.81%	Nil	Nil

moderately polluted for As and Cd respectively, while Cd fell under uncontaminated to moderately contaminated class in 14.29% of the sediment samples.

During the wet season, the trend of Igeo values was observed to be different from the previous season. This time, the Igeo values of Pb, Ni, Cr, Zn, Co, Al, Cu and As exhibited extreme high pollution in the sediment samples. On the other hand, Igeo values for Cd revealed that 23.81% of the samples could be classified under strongly polluted, 33.33% under moderately to strongly polluted, 38.1% under moderately polluted, and 4.76% under strongly to extremely polluted. Based on the overall evaluation using the Muller scale, the results conclude that most of the sediment samples were classified as strongly to extremely polluted for all metal(oid), except for Cd and As which showed inconsistent variation among the Muller classification.

3.3.4. Potential ecological risk index

The outcome of PERI assessment for the different seasons (dry and wet) are presented in Fig. S2. The PERI values obtained during the dry season revealed that the ecological integrity of the sample region had been compromised. High ecological risk was observed in 19.11% of the investigated samples, considerable ecological risk was observed in 66.67% of the samples, and 14.33% of the samples were grouped under moderate ecological risk. Considering this, As and Cd are the highest contributors to the ecological risk experienced within the river for both seasons. In the wet season, we observed further reduction of the ecological quality of the area as 85.67% of the investigated samples produced high ecological risk

Table 3
Igeo representation according to sample location during the dry and wet season.

Sample ID	Igeo > 5	4< Igeo ≤ 5	3< Igeo ≤ 4	2< Igeo ≤ 3	1< Igeo ≤ 2	0< Igeo ≤ 1
Dry Season						
SMP1	Pb, Ni, Cr, Zn, Co, Al, Cu	–	–	–	As	Cd
SMP2	“	–	–	–	As, Cd	–
SMP3	“	–	–	–	As, Cd	–
SMP4	“	–	–	As, Cd	–	–
SMP5	“	–	–	As, Cd	–	–
SMP6	“	–	–	As, Cd	–	–
SMP7	“	–	–	As	Cd	–
SMP8	“	–	–	As	Cd	–
SMP9	“	–	As	–	Cd	–
SMP10	“	–	–	Cd	As	–
SMP11	“	–	–	Cd	As	–
SMP12	“	–	–	Cd	As	–
SMP13	“	–	As	–	Cd	–
SMP14	“	–	–	As	Cd	–
SMP15	“	–	As	–	–	Cd
SMP16	“	–	–	As	Cd	–
SMP17	“	–	As	–	–	Cd
SMP18	“	–	As	–	Cd	–
SMP19	“	–	Cd	As	–	–
SMP20	“	–	Cd	As	–	–
SMP21	“	–	–	Cd, As	–	–
Wet Season						
SMP1	Pb, Ni, Cr, Zn, Co, Al, Cu, As	–	–	–	Cd	–
SMP2	“	–	–	–	Cd	–
SMP3	“	–	–	–	Cd	–
SMP4	“	–	Cd	–	–	–
SMP5	“	–	Cd	–	–	–
SMP6	“	–	Cd	–	–	–
SMP7	“	–	–	Cd	–	–
SMP8	“	–	–	–	Cd	–
SMP9	“	–	–	–	Cd	–
SMP10	“	–	–	Cd	–	–
SMP11	“	–	–	Cd	–	–
SMP12	“	–	–	Cd	–	–
SMP13	“	–	–	Cd	–	–
SMP14	“	–	–	–	Cd	–
SMP15	“	–	–	–	Cd	–
SMP16	“	–	–	Cd	–	–
SMP17	“	–	–	–	Cd	–
SMP18	“	–	–	Cd	–	–
SMP19	“	Cd	–	–	–	–
SMP20	“	–	Cd	–	–	–
SMP21	“	–	Cd	–	–	–

values, while 14.33% of the samples fell under the considerable ecological risk zone. The pollution intensities emanating from these sites indicated that Cd and As added the largest proportion considering that Cd emissions originate from human activities. This implies that there exists a severe threat on the biological community of River Atuwara caused by the combined action of As and Cd.

3.3.5. Toxic risk index (TRI)

A complimentary assessment known as the toxic risk index (TRI) was adopted to provide a more detailed measurement of their risk to the biota in the river environment. To ascertain the TRI, we combined the results obtained from both seasons (dry and wet season) to estimate the potential toxicity of the individual metal(-oid) in the ecosystem. Applying the aforementioned index, the Mean ± SD TRI value for Cu (2.641 ± 0.9691), As (1.213 ± 0.5623), Cd (4.088 ± 2.447), Pb (0.7809 ± 0.4193), Ni (2.044 ± 1.652), Cr (0.5136 ± 0.17), and Zn (1.121 ± 0.4793) were obtained. Considering the mean value, it could be deduced that there is no risk posed by the metal(oid)s. However, attention should be directed at Cd because of the heightened TRI values in SMP14 and SMP15 (Fig. S3a).

Interestingly, the result of the TRI at SMP14 and SMP15 is not surprising as few meters away from SMP15 lies an abattoir that deposits abattoir sludge around the river banks. Sludge deposition can also generate anoxic conditions that favour the precipitation of metal(oid)s and this might be responsible for the high occurrence of metal(oid)s, especially Cd in the sediment sample obtained at SMP14. In addition, TRI values of Ni indicated low risk at SMP8 and SMP9, and Cd at SMP4, SMP6, and SMP21. The spatial representation of the TRI values for Ni revealed an increase in toxicity in the south and northwest region of the study area (Fig. 3a-g). Meanwhile, the spatial map of the Cd TRI showcases high toxicity in the northern and southern region of the study area (Fig. 3c). The implication of this reveals the region that is characterized by high anthropogenic activities around River Atuwara.

To add, we adopted a recently proposed pollution index related to the degree of contamination—The modified Hazard Quotient (mHQ). The mHQ assesses levels of contamination by describing each metal(oid) concentration found in the sediment with the threshold limits of adverse ecological distributions such as the SEL, PEL and TEL. The evaluation of mHQ is of utmost importance since it evaluates the risk of individual metal(oid)s to the biota and the aquatic environment (Benson et al., 2018).

With respect to the mHQ values obtained, Cd contamination in the samples could be grouped between considerable severity to extreme severity. Concerning Ni contamination, a few samples

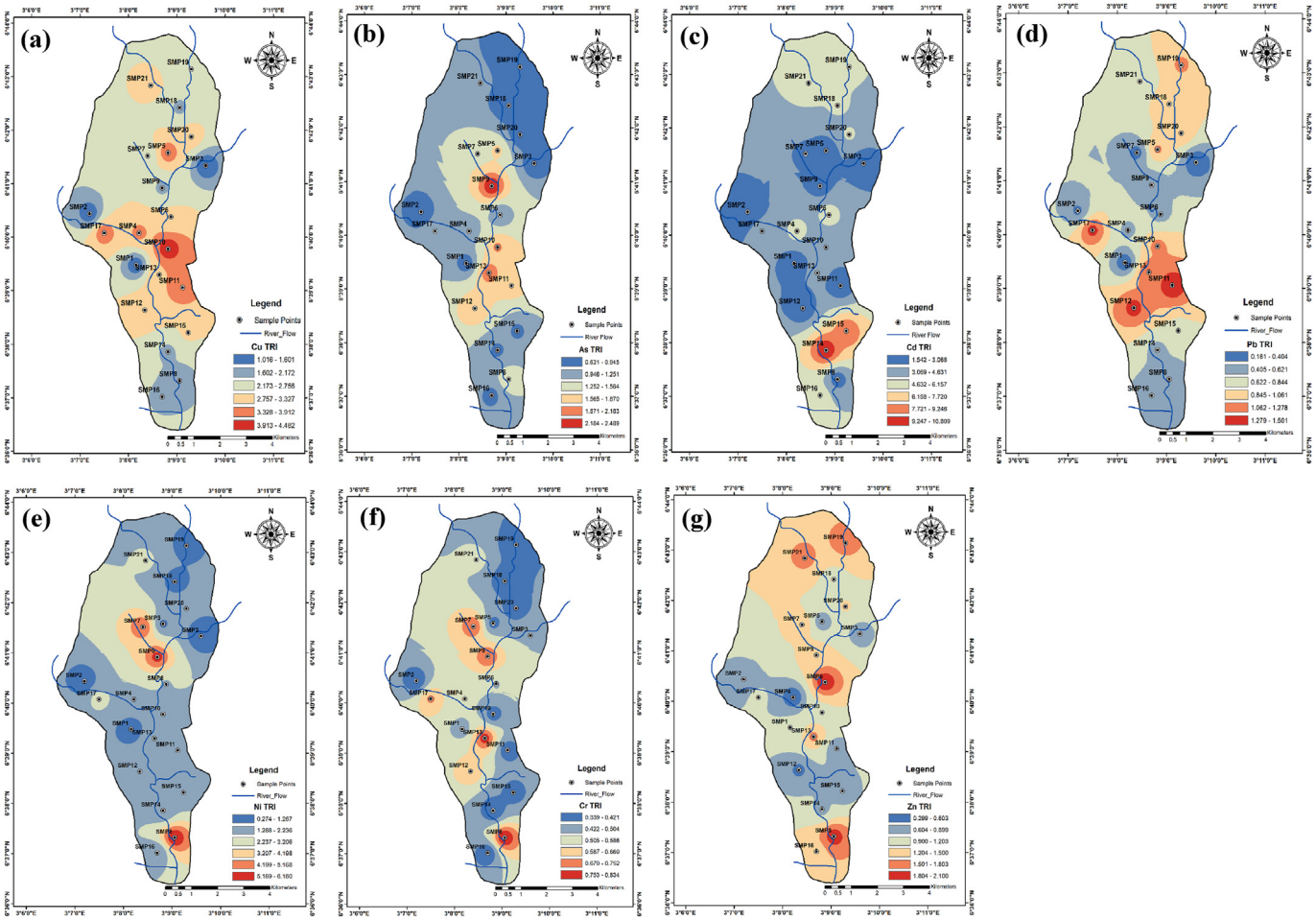

Fig. 3. Spatial distribution of Toxic Risk Index (TRI) for (a) Cu (b) As (c) Cd (d) Pb (e) Ni (f) Cr (g) Zn.

(14.29%) fell under very high severity, 38.09% categorized as moderate severity, 23.81% classified as low severity, and 14.29% as very low severity (Fig. S3b). Further insight to Cu contamination revealed considerable severity in 38.09% of the samples and moderate severity in 47.62% of the samples. As contamination fell under three categories of mHQ rating; 38.1% as moderate severity contamination, 52.38% as low severity contamination, and 9.52% as very low severity contamination. Pb contamination recorded 47.62% as low severity and 52.38% as very low severity. Meanwhile, the spatial map of the mHQ is represented in (Fig. 4a-g).

3.4. Multivariate compositional assessment of the sediment data

3.4.1. Source identification using PC/FA

After obtaining the centered log-transformed data, Principal Component/Factor Analysis (PC/FA) was used to explain the inter-variable relationship, Euclidean discrepancies, and potential origin in relation to the geochemical pattern. Varimax rotation combined with communality technique was used to support the PC/FA to obtain a simplified expression of the variables without altering the coordinate pattern of the variables.

In total, five factors were selected (based on the 1-mark breakpoint of the scree-graph), which accounts for 88.41% and 88.06% of the data variability during the dry and wet season, respectively. The extracted factors for the dry season, identified as E1, E2, E3, E4, and E5, accounts for 31.03%, 20.23%, 14.82%, 12.20%, and 10.13% variability, respectively. For the wet season dataset, the five factors represented as F1, F2, F3, F4, and F5 accounts for 30.80%, 20.85%, 14.41%, 11.86%, and 10.14% variability, respectively (Tables S3(a–b)). For the current study, we considered variables with loadings greater than 0.5 as an adequate representative of the main factor composition.

Considering the biplot of the Clr-transformed data, it is vital to identify the groupings of variables falling side-by-side and the weight of their loading before documenting the observations. In Fig. 5a-b, E1 is characterized by high loadings from As, Ni, Cu, Cr, Al, and Pb. The association is dominated by As (0.8468), with communality of 82.17%, and the elemental association reflects the mixing of human and industrial activities within the river basin. Potential sources such as biosolids (municipal sewage sludge, livestock manure, and compost) and wood industries might be responsible for the accumulation of the listed metal(oid)s in the sediments (Basta et al., 2005; Emenike et al., 2019a, 2019b; Wuana and Okieimen, 2011). E2 is associated with high positive loadings from Cu and Pb, which are characteristics of pollution sources emanating from plastic industry and industrial effluents. Apparently, these are everyday happenings around the study area as industries located within the vicinity consider River Atuwara as a dumping spot for their effluent wastewater (Tenebe et al., 2018). E3 is observed to have high loadings from Co (0.6207) and Zn (0.5548), indicating possible derivation from lithological content. However, it has been reported that the values of Zn surpassing 800 mg/kg in sediments denote the impact of metalliferous mining (Emenike et al., 2018; Maanan et al., 2015). E4 receives high positive

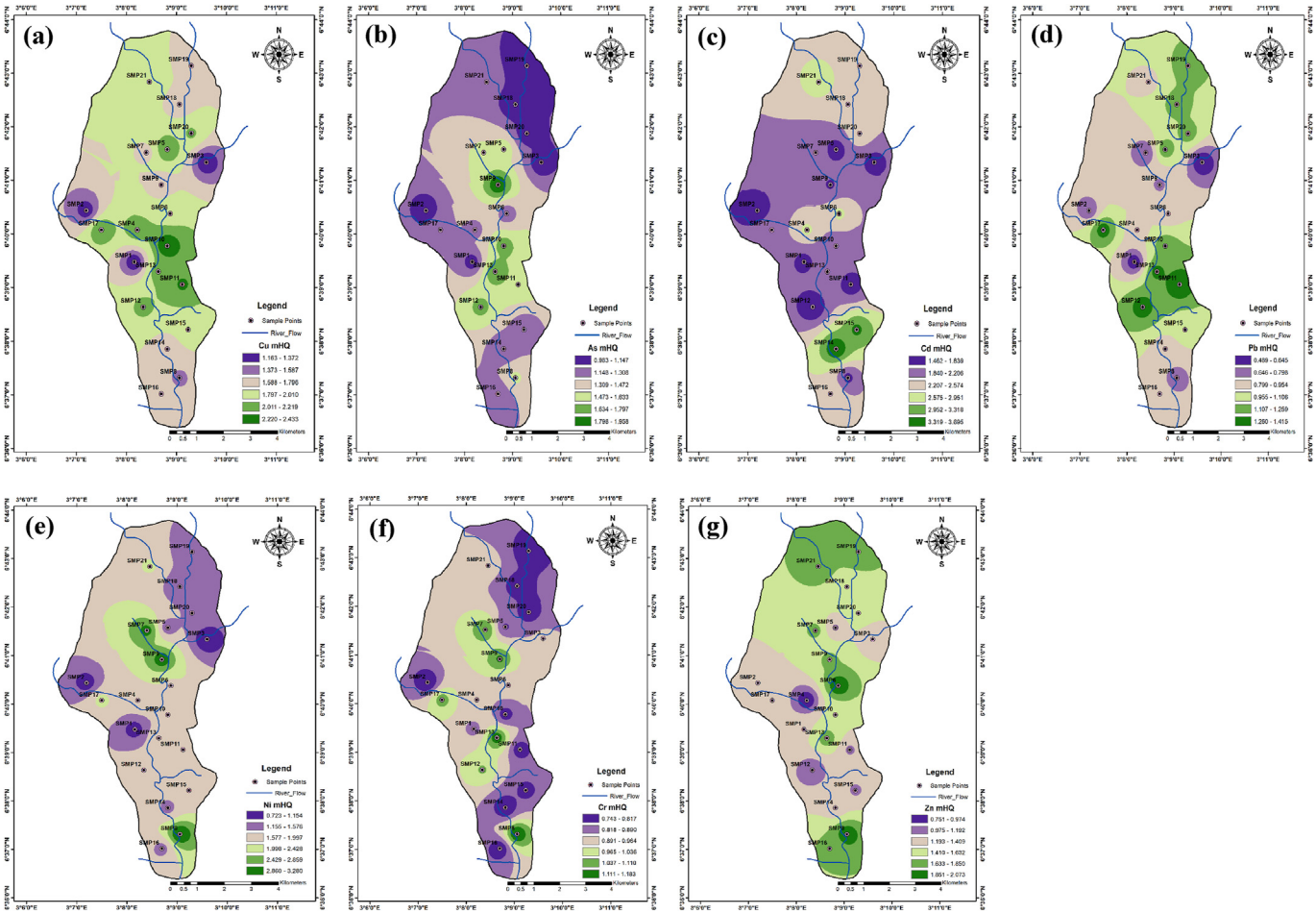

Fig. 4. Spatial distribution of Modified Hazard Quotient (mHQ) for (a) Cu (b) As (c) Cd (d) Pb (e) Ni (f) Cr (g) Zn.

loading from standalone Cd variable (0.6179), probably originating from an anthropogenic source e.g. high traffic and combustion of fossil fuels (Mama et al., 2020; Obiora et al., 2016). Considering the impact of land use, there is a possibility that high vehicular movement contributes a significant amount of environmental pollutants to the river basin (Mukhopadhyay et al., 2016). E5 is characterized by high positive loading from Fe (0.8096), implying that there are traces of pyroclastic deposits which is associated with Fe–Mn-Oxy-hydroxide precipitation in siliciclastic accumulations (Zuzolo et al., 2017).

From the dataset obtained in the wet season, we observed a consistent trend in Factor 1 (F1) similar to E1 obtained from the dry season (Fig. 5c-d). However, F2 recorded high positive loading from Cu (0.7029) and Pb (0.6218) and a high negative loading from Co (−0.5827). This association is linked to a possible blend of organic matter content superimposed on lithological attributes (Emenike et al., 2020a, 2020b; Tolosana-Delgado and McKinley, 2016). F3 is characterized with high positive loadings from Zn (0.6431), Co (0.5192), and Cd (0.5011). This association is linked to possible pollution from paint and dye industries (Shen et al., 2017). The loading on F4 and F5 is similar to E4 and E5, implying a potential reoccurring source as indicated in the dry season.

3.4.2. Constellation analysis of Clr-transformed data

The constellation plot (C-Plot) of the Clr-transformed was obtained using the Ward method with Euclidean distance. It highlights the relationship of the variables in Euclidean geometry and identifies variables based on their probable interaction of geochemical origin. In Fig. 5e, three clusters were identified, having associations between Fe–As–Cr–Co–Ni–Zn–Al (Cluster 1), Cu–Pb (Cluster 2), and Cd (Cluster 3) in the dry season. Cluster 1, having an association between Fe–Al–Zn–Co, is related to lithogenic contribution, while As–Ni–Cr is related to chemicals used for wood treatment. From cluster 1, it is evident that the lithogenic pollution are the dominant contributors of the toxic metal(oid)s highlighted (Brady et al., 2014a; Saleem et al., 2015). Cluster 2, with Cu–Pb association, is synonymous to chemicals from antifouling paints and traffic emissions (Brady et al., 2014b; Pulles et al., 2012). Cluster 3 pinpointed Cd, which is related to the deposition of industrial waste.

In the wet season, three clusters were also identified as having associations between Cu–Pb–As–Ni (Cluster 1), Cr–Fe–Al–Zn–Co (Cluster 2), and Cd (Cluster 3) (Fig. 5f). Cluster 1 supports the view that the metal(oid)s share a common source, inferring possible impact from an anthropogenic medium such as sludge accumulation from abattoirs, metal smelting and industrial discharge. Cluster 2 infers potential contribution from natural origin. In corroboration, dredging activities occurring in River Atuwara might be the possible reason why these parent metal(oid)s are identified in the sediments (Bancon-Montigny et al., 2019). Cluster 3 is consistent with the association observed during the dry season.

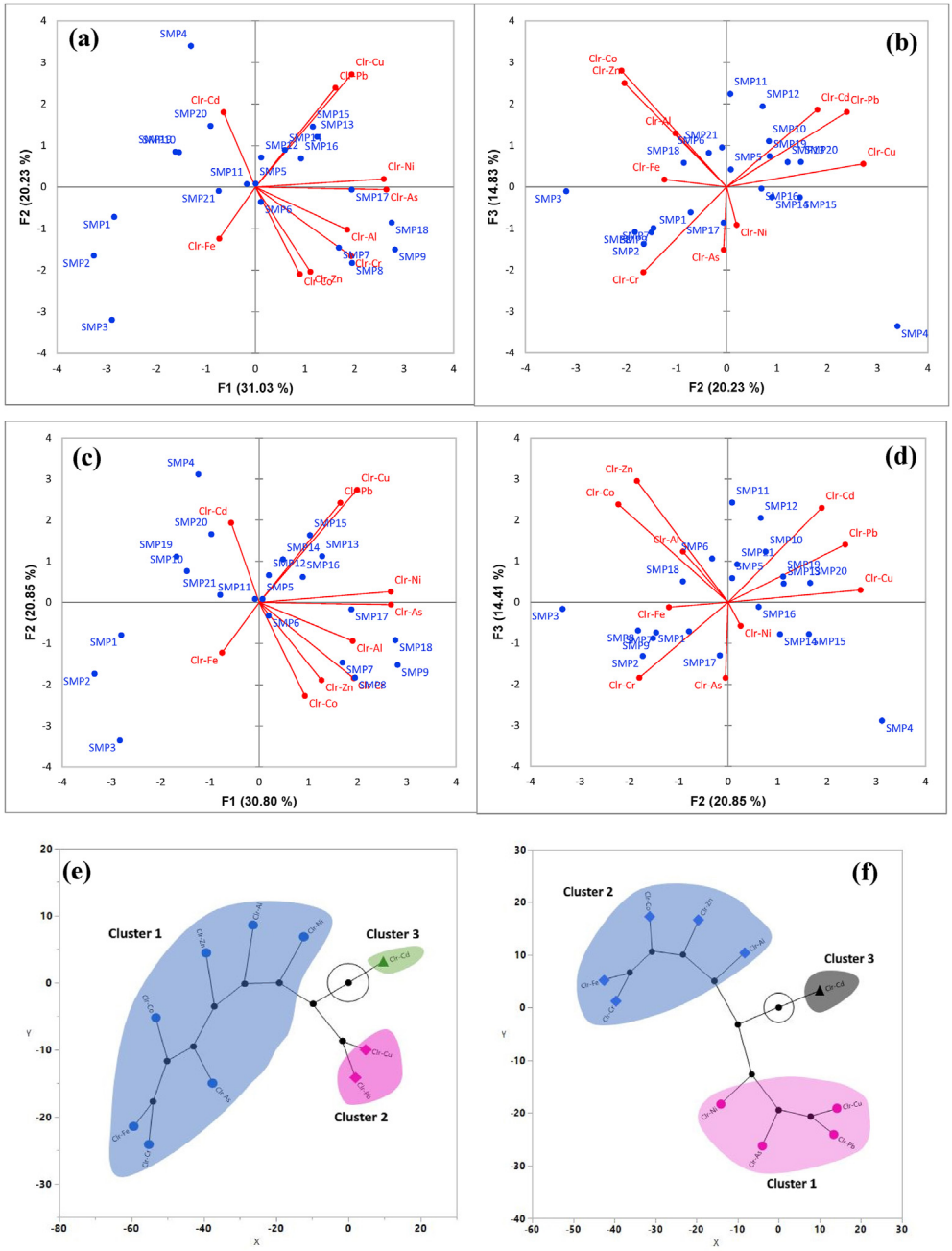

Fig. 5. Multivariate Statistical representation of metal(oid)s in sediments (a) Biplot of factor 1 vs 2 (b) Biplot of factor 2 vs 3 in the dry season (c) Biplot of factor 1 vs 2 (d) Biplot of factor 2 vs 3 in the wet season (e) C-Plot indicating metal(oid) cluster in the dry season (f) C-Plot indicating metal(oid) cluster in the wet season.

3.5. Human health risk assessment

The HRA results obtained for residential scenario were rated according to the safety mark outlined by the USEPA for children and adult considering the ingestion and dermal pathway through the sampling location. For non-cancer risk via the ingestion route, the aggregated HI varied from 5.40E−1 to 2.95E+00 (mean value of 1.81E+00) for children and 5.06E−2 to 2.77E−1 (mean value of 1.70E−1). The results presented a higher aggregated HI during the wet season and exceeded the safety standard as the values ranged from 1.14E+00 to 3.50E+00 for children. The aggregated HI values obtained for adults were within the stipulated standard ($HI \leq 1$), as the values varied from 1.07E−1 to 3.28E−1 (mean values of 2.20E−1). After evaluating the mean HI increment for both seasons, the cumulative HI for adults during the wet season increased by 1.29 times the value obtained during the dry season, whereas the cumulative mean HI for children during the wet season surpassed that of the dry season by 1.4 times.

Furthermore, the highest cumulative non-cancer risk for children and adult considering both seasons ensued at SMP8, followed by SMP17, SMP13, SMP16, and SMP9, respectively. These values exceeded the safe threshold by more than 100% during the wet season, implying that, children are likely to develop adverse non-carcinogenic health effect, especially for those living in close proximity to River Atuwara. However, it is noteworthy to mention that sediments might not be the only route to ingest cancer-causing

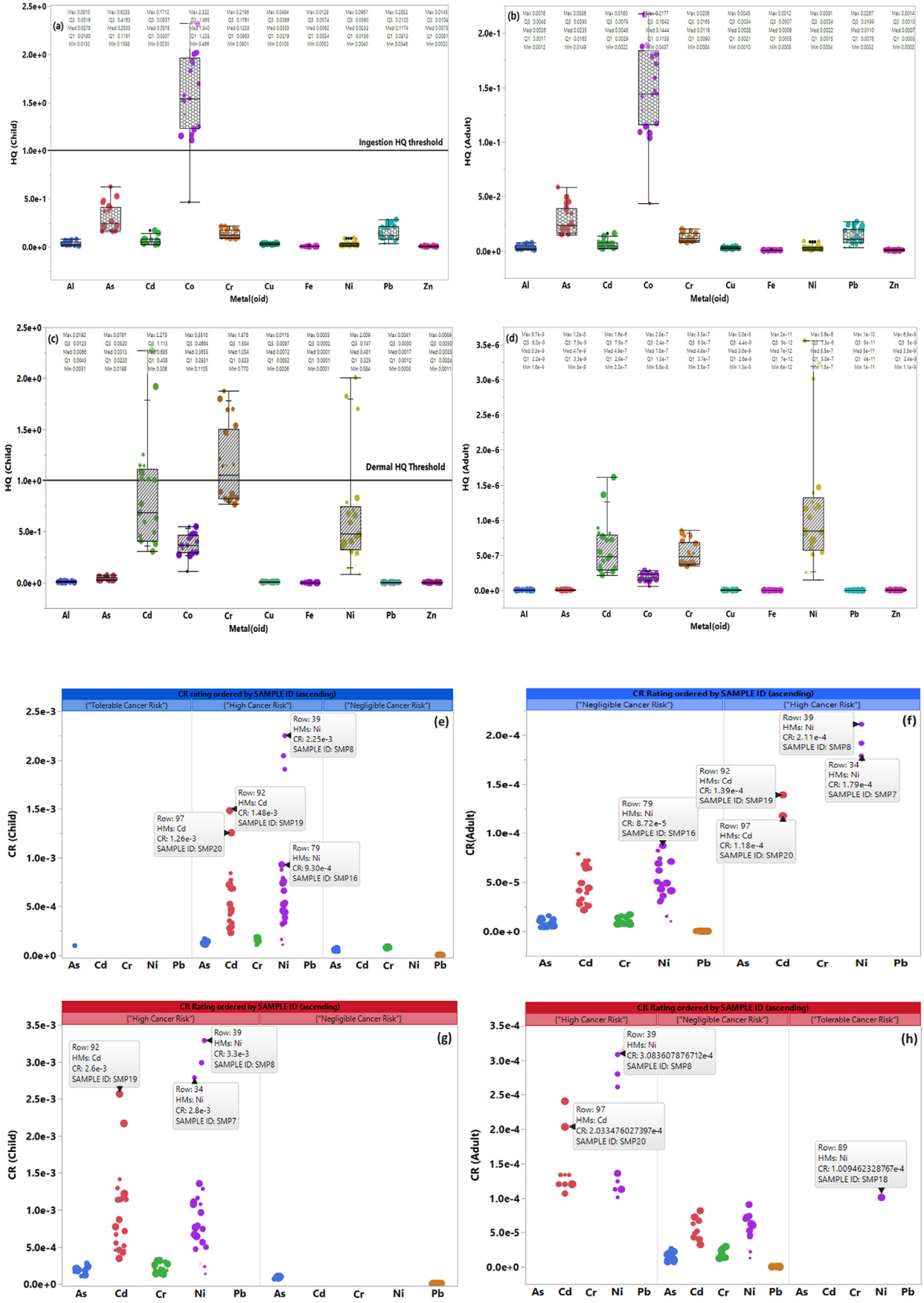
(a)
HQ (Child)
Ingestion HQ threshold
Metal(oid)
Al As Cd Co Cr Cu Fe Ni Pb Zn
(b)
HQ (Adult)
Metal(oid)
(c)
HQ (Child)
Dermal HQ Threshold
Metal(oid)
(d)
HQ (Adult)
Metal(oid)
CR rating ordered by SAMPLE ID (ascending)
{"Tolerable Cancer Risk"} {"High Cancer Risk"} {"Negligible Cancer Risk"}
(e)
CR (Child)
Row: 39 HMs: Ni CR: 2.25e-3 SAMPLE ID: SMP8
Row: 92 HMs: Cd CR: 1.48e-3 SAMPLE ID: SMP19
Row: 97 HMs: Cd CR: 1.26e-3 SAMPLE ID: SMP20
Row: 79 HMs: Ni CR: 9.30e-4 SAMPLE ID: SMP16
CR Rating ordered by SAMPLE ID (ascending)
{"Negligible Cancer Risk"} {"High Cancer Risk"}
(f)
CR(Adult)
Row: 39 HMs: Ni CR: 2.11e-4 SAMPLE ID: SMP8
Row: 34 HMs: Ni CR: 1.79e-4 SAMPLE ID: SMP7
Row: 92 HMs: Cd CR: 1.39e-4 SAMPLE ID: SMP19
Row: 79 HMs: Ni CR: 8.72e-5 SAMPLE ID: SMP16
Row: 97 HMs: Cd CR: 1.18e-4 SAMPLE ID: SMP20
CR Rating ordered by SAMPLE ID (ascending)
{"High Cancer Risk"} {"Negligible Cancer Risk"}
(g)
CR (Child)
Row: 92 HMs: Cd CR: 2.6e-3 SAMPLE ID: SMP19
Row: 39 HMs: Ni CR: 3.3e-3 SAMPLE ID: SMP8
Row: 34 HMs: Ni CR: 2.8e-3 SAMPLE ID: SMP7
CR Rating ordered by SAMPLE ID (ascending)
{"High Cancer Risk"} {"Negligible Cancer Risk"} {"Tolerable Cancer Risk"}
(h)
CR (Adult)
Row: 39 HMs: Ni CR: 3.083607876712e-4 SAMPLE ID: SMP8
Row: 97 HMs: Cd CR: 2.033476027397e-4 SAMPLE ID: SMP20
Row: 89 HMs: Ni CR: 1.009462328767e-4 SAMPLE ID: SMP18

trace elements. Taking into account the metal-specific HQ, Cobalt was observed to be the most significant contributor to the overall HI. For children, the HQ of cobalt exceeded the safety limit of 1 for all samples (Fig. 6a), whereas, for adults, the values were within the stipulated standard (Fig. 6b). Apart from the high HQ observed for Co, the contribution of chemical species towards the overall HQ are in order of As $\gg$ Pb > Cr > Cd > Al > Ni > Cu > Zn > Fe throughout the dry and wet season.

Concerning the non-cancer risk via dermal route, the HQ of Cr, Cd, and Ni exceeded the safe condition for children during the wet season but remained within limits for adults. The HQ_{child} obtained during the wet season were high for Cr in 52.38% of the samples, Cd in 42.86% of the samples, and Ni in 14.29% of the samples (Fig. 6c). High HQ_{child} observed for Cr had the highest contribution emanating from SMP8, followed by SMP18. For Cd, the highest value of HQ_{child} was reported at SMP19 and SMP20, while for Ni, SMP8 had the highest value. The HQ obtained for adults during the wet season were below the safe limits. However, the average metal-specific HQ values were in order of Ni > Cd > Cr > Co > As > Al > Zn > Cu > Pb > Fe (Fig. 6d). The implication of this reflects on the potential hazard derived from multiple metal(oid)s in which children are exposed to within the sample region. Also, it is important to note that the intake of high concentration of Cr may result in nasal, sinus, and lung cancer. Excessive intake of Cd causes renal dysfunction, and lung impairment (leading to cancer of the lungs), whereas high amounts of Ni in the body result in chronic bronchitis (ASTDR, 2005; ATSDR, 2008; NCM, 2003). Considering all of these, priority should be directed at the population within the adolescent age-grade living within the study region to safeguard their living conditions.

According to the HRA calculation conducted during the dry season, we observed a reduced risk for children via dermal pathway. Although the HQ values for some sites surpassed 1 for specific metal(oid)s, the values were reduced compared to the HRA conducted during the wet season. For children, high HQ values exceeding the threshold were observed for Cd at SMP19 and SMP20, for Ni at SMP8, SMP10, and SMP9, and for Cr at SMP8 and SMP18. For adults, we observed minimal values far less than the safe limit (see supplementary material). In Total, the aggregated HI for adult ranged from 6.99E−7 to 3.30E−6, whereas the cumulative HI for children surpassed the safe standard, varying between 1.06E+00 to 3.09E+00 (average value of 1.97E+00).

In the current work, we estimated and categorized the cancer risk of five metal(oid)s based on the classification (CR > 1×10^{-4} = High Risk; CR of 1×10^{-6} to 1×10^{-4} = Tolerable Risk; CR < 1×10^{-6} = Negligible Risk) proposed by Wu et al. (2015) (See Fig. 7). From the results obtained, the CR for children via ingestion route indicated a high cancer risk for As, Cd, Cr, and Ni during the dry season; a tolerable risk for As, and a negligible risk for As, Cd, and Pb (Fig. 6e). For adults, the CR via ingestion revealed a negligible risk for all metal(oid)s at most of the sampled locations; high risk for Cd and Ni at SMP19, SMP20, SMP8, SMP9, and SMP7 respectively (Fig. 6f). During the wet season, we observed a potential high cancer risk for As, Cd, Cr, and Ni for children via ingestion route. However, heightened values observed for Ni and Cd occurred at SMP8 and SMP19, respectively (Fig. 6g). For adults, most locations were grouped under negligible risk in relation to all metal(oid)s. SMP18 is classified under tolerable risk related to Ni, while a few locations were categorized under high risk associated with Ni and Cd (Fig. 6h).

In general, Ni and Cd posed a severe detrimental threat to human lives living within the vicinity of River Atuwara. The risks identified are linked to the pollution arising from the unwarranted discharge of wastewater. Therefore, environmental management authorities must consider this study as a wake-up call to revive the ecological quality of River Atuwara. The current study advocates for more stringent legislation as a foundational step to halt environmental pollution within Ado-Odo Ota since the region is popular as an industrial settlement. Other results related to the CR via dermal route is located in the supplementary section (See Tables S4 and S5 in the Supplementary material).

4. Conclusion

Based on the current investigation, levels of potentially toxic elements in sediments of River Atuwara exceeded some of the sediment quality guidelines signifying a varying degree of contamination. The concentration of Ni, Cr, As, Pb, Cd and Co were elevated in most sediment samples. Further explanation indicated that the mean concentration of the selected toxic elements in the sediments obtained from River Atuwara followed the increasing order of Cd < As < Cr < Pb < Co < Ni < Cu < Zn < Fe < Al in the dry season and an increasing order of Cd < As < Cr < Co < Pb < Ni < Cu < Zn < Fe < Al during the wet season. The LULC highlighted the impact of urbanization, vegetation loss and industrialization as possible contributors of anthropogenic pollutants. Source apportionment was achieved using the center log-transformed approach linked with compositional data analysis. The outcome of the log-transformed PC/FA and constellation plot analysis indicated biosolids, lithological content, vehicular activities and industrial actions as the reason for contamination. Analysis of sediments samples with different pollution and ecological indices revealed that pollution was higher in the wet season than in the dry season with Cd and As contributing a larger fraction of proportion.

The EF values in the dry season identified minimal enrichment for majority of the metal(oid)s investigated in more than 52% of the samples; moderate enrichment for Zñ 48%, As ~ 48%, Ni, Co, Cr ~ 48%, Cd in ~10%, and significant enrichment for As in ~39% of the samples. EF in the wet season revealed moderate enrichment for As, Cd, Co, Cr, Cu, Ni, Pb, and Zn in 23.81%, 42.86%, 33.33%, 61.90%, 28.57%, 4.76%, 14.28%, and 52.38% of the samples, and significant enrichment for As, Cr, Ni in 76.19%, 4.76%, and 9.52% of the samples, respectively. Further insights to the pollution status obtained from the PLI rating indicated that 90.48% of the sediment samples in the riparian area of River Atuwara are polluted by the metal(oid)s investigated. The Igeo identified that most of the sediment samples are extremely polluted with the metal(oid)s considered in this study; however, inconsistent variations were observed for Cd and As. The rating derived from the ecological risk index depicted that the highest proportion of ecological risk within the study region is caused by Cd and As. Meanwhile the TRI assessment disclosed that Cd poses a higher risk, particularly around the northern and southern part of the study area. Taking into consideration the sediment quality guidelines, mHQ rating revealed that there is very high and moderate severity of Ni contamination in 14.29% and 38.09% of the samples, considerable and moderate severity of Cu contamination in 38.09% and 47.62% of the samples, and moderate severity of As contamination in 47.62% of the samples, respectively.

Fig. 6. Characterization of (a) HQ for children via ingestion pathway(b) HQ for adults via ingestion pathway (c) HQ for children via dermal pathway (d) HQ for adult via dermal pathway; during the wet season (e) CR for children during the dry season (f) CR for adults during the dry season (g) CR for children via during the wet season (h) Cr for adult during the wet season; via ingestion pathway.

The HRA of metal(oid)s and aggregated HI observed at SMP8 was very high for both adults and children. Considering the mean HI, the incremental risk posed by toxic elements were higher for children than adults. At some location (SMP8, SMP17, SMP13, SMP16, and SMP9), the non-cancer risk for children via ingestion pathway exceeded the safe limit by more than 100% during the wet season. This implies that children are more susceptible to the hazards posed by metal(oid)s than adults within the vicinity of River Atuwara. Regarding the metal-specific HQ via ingestion route, the risks are in order of Co ≫ As ≫ Pb > Cr > Cd > Al > Ni > Cu > Zn > Fe throughout the dry and wet seasons. Also, the dermal non-cancer risk of specific toxic metal(oid)s such as Cr, Cd, and Ni exceeded the safe limit for children during the wet season. However, the average metal-specific HQ values were in order of Ni > Cd > Cr > Co > As > Al > Zn > Cu > Pb > Fe.

The carcinogenic risk for children via ingestion route presented high values for As, Cd, Cr, and Ni during both seasons. However, a severe critical case was observed at SMP8 and SMP19 in which the CR posed by Ni and Cd were far beyond limits. Overall, Ni and Cd posed a severe threat and contributed more to the CR values observed. Thus, the study suggests legislative and regulatory revamp, investigative co-operation, incorporation of pollution indices and risk assessment into environmental management strategies, and stringent implementation of environmental laws since river sediments hold vital information on the combined impact of human activities and climate change within a river basin.

Declaration of competing interest

The authors declare that they have no known competing financial interests or personal relationships that could have appeared to influence the work reported in this paper.

CRediT authorship contribution statement

PraiseGod Chidozie Emenike: Funding acquisition, Conceptualization, Investigation, Software, Writing - original draft, Resources. **Imokhai Theophilus Tenebe:** Investigation, Data curation, Formal analysis, Resources. **Jordan Brizi Neris:** Data curation, Software, Formal analysis. **David Olugbenga Omole:** Investigation, Writing - review & editing, Formal analysis. **Olaniyi Afolayan:** Formal analysis, Data curation, Writing - review & editing. **Chukwueloka Udechukwu Okeke:** Writing - review & editing, Validation. **Ikechukwu Kingsley Emenike:** Investigation, Resources.

Acknowledgement

This work was supported by the Commonwealth Scholarship Commission, United Kingdom (Grant number NGCN-2017-57).

Appendix 1

$$CDI_{sed-Derm-nc-ad} = \frac{C_{sed}\left(\frac{mg}{kg}\right) \times EF_{ad}\left(\frac{350\ days}{year}\right) \times ED_{ad}(26years) \times SA_{ad}\left(\frac{6032\ cm^2}{day}\right) \times AF_{ad}\left(\frac{0.07\ mg}{cm^2}\right) \times ABS_{derm} \times \left(\frac{10^{-6}kg}{1\ mg}\right)}{AT_{ad}\left(\frac{365\ days}{year} \times ED_{ad}\right) \times BW_{ad}(80\ kg)} \tag{11}$$

$$CDI_{sed-Ing-nc-ad} = \frac{C_{sed}\left(\frac{mg}{kg}\right) \times EF_{ad}\left(\frac{350days}{year}\right) \times ED_{ad}(26years) \times InR_{ad}\left(\frac{100\ mg}{day}\right) \times RBA \times \left(\frac{10^{-6}kg}{1\ mg}\right)}{AT_{ad}\left(\frac{365\ days}{year} \times ED_{ad}\right) \times BW_{ad}(80kg)} \tag{12}$$

$$CDI_{sed-Derm-nc-ch} = \frac{C_{sed}\left(\frac{mg}{kg}\right) \times EF_{ch}\left(\frac{350\ days}{year}\right) \times ED_{ch}(6years) \times SA_{ch}\left(\frac{2373\ cm^2}{day}\right) \times AF_{ch}\left(\frac{0.2\ mg}{cm^2}\right) \times ABS_{derm} \times \left(\frac{10^{-6}kg}{1\ mg}\right)}{AT_{ch}\left(\frac{365\ days}{year} \times ED_{ch}\right) \times BW_{ch}(15\ kg)} \tag{13}$$

$$CDI_{sed-Ing-nc-ch} = \frac{C_{sed}\left(\frac{mg}{kg}\right) \times EF_{ch}\left(\frac{350\ days}{year}\right) \times ED_{ch}(6years) \times InR_{ch}\left(\frac{200\ mg}{day}\right) \times RBA \times \left(\frac{10^{-6}kg}{1\ mg}\right)}{AT_{ch}\left(\frac{365\ days}{year} \times ED_{ch}\right) \times BW_{ch}(15\ kg)} \tag{14}$$

$$HQ_{ch,ad-Ing} = \frac{CDI_{sed-Ing-ch,ad}}{RfD_o} \tag{15}$$

$$RfD_{ABS} = RfD_o \times ABS_{GI} \tag{16}$$

$$HQ_{ch,ad-Derm} = \frac{CDI_{sed-Derm-ch,ad}}{RfD_{ABS}} \tag{17}$$

$$CR_{Ing} = CDI_{sed-Ing-ch,ad} \times SF_o \; ; CR_{Derm} = CDI_{sed-Derm-ch,ad} \times SF_{ABS}$$
$$\text{where } SF_{ABS} = \frac{SF_o}{ABS_{GI}} \tag{18}$$

Nomenclature

ABS_{Derm}	Dermal absorption factor
ABS_{GI}	Fraction of contaminant absorbed in gastrointestinal tract
AF_{ad}	Soil adherence factor for adult (mg cm-^{2})
AF_{ch}	Soil adherence factor for child (mg cm-^{2})
AT_{ad}	Averaging time for adult (days)
AT_{ch}	Averaging time for child (days
BW_{ad}	Body weight for adult (kg)
BW_{ch}	Body weight for child (kg)
C_{sed}	Concentration of metal(oid) in sediment (mg kg^{-1})
$CDI_{sed-Ing-nc-ch}$	Chronic daily intake of sediment via ingestion exposure route (child) (mg kg-1 d-1)
$CDI_{sed-Derm-nc-ch}$	Chronic daily intake of sediment via dermal exposure route (child) (mg kg^{-1} d^{-1})
$CDI_{sed-Ing-nc-ad}$	Chronic daily intake of sediment via ingestion exposure route (adult) (mg kg^{-1} d^{-1})
$CDI_{sed-Derm-nc-ad}$	Chronic daily intake of sediment via dermal exposure route (adult/child) (mg kg^{-1} d^{-1})
CF	Conversion factor (kg mg^{-1})
CR_{Ing}	Cancer Risk via ingestion exposure route
CR_{Derm}	Cancer risk via dermal exposure route
ED_{ad}	exposure duration for adult (years)
ED_{ch}	exposure duration for child (years)
EF_{ad}	Exposure frequency for adult (days year^{-1})
EF_{ch}	Exposure frequency for child (days year^{-1})
$HQ_{ch,ad-Ing}$	Hazard Quotient via ingestion exposure route (adult/child)
$HQ_{ch,ad-Derm}$	Hazard Quotient via dermal exposure route (adult/child)
InR_{ad}	Intake rate for adult (mg day^{-1})
InR_{ch}	Intake rate for child (mg day^{-1})
RBA	Relative Bioavailability Factor
RfD_{ABS}	Dermal oral reference dose (mg kg^{-1} d^{-1})
RfD_o	Ingestion oral reference dose (mg kg^{-1} d^{-1})
SA_{ad}	Skin surface area for adult (cm^2 day^{-1})
SA_{ch}	Skin surface area for child (cm^2 day^{-1})
SF_{ABS}	Dermal slope factor (mg kg^{-1} d^{-1})$^{-1}$
SF_o	Ingestion slope factor (mg kg^{-1} d^{-1})$^{-1}$

The values of RfD_O, ABS, ABS_{GI}, SF_O, and RBA for specific metal(-oid) are presented in the supplementary material (Table S6).

Appendix A. Supplementary data

Supplementary data to this article can be found online at https://doi.org/10.1016/j.envpol.2020.114795.

References

Aboud, J.S., Nandini, N., 2009. Impact assessment of heavy metals pollution of Vartur lake, Bangalore. J. Appl. Nat. Sci. 1, 53–61. https://doi.org/10.31018/jans.v1i1.35.

Adewumi, I.K., Ogbiye, A.S., Longe, E., Omole, D., 2011. Effect of industrial effluents on water quality of river Atuwara in Ota , Nigeria: in urban agriculture, cities and climate change. In: Urban Agriculture, Cities and Climate Change. Cuvillier Verlag Gottingen, pp. 272–280.

Aitchison, J., 1999. Logratios and natural laws in compositional data analysis. Math. Geol. 31, 563–580. https://doi.org/10.1023/A:1007568008032.

Aitchison, J., 1982. The statistical analysis of compositional data the statistical analysis of compositional data. J. ofthe R. Stat. Soc. Ser. B 44, 139–177.

Akhbarizadeh, R., Moore, F., Keshavarzi, B., Moeinpour, A., 2017. Microplastics and potentially toxic elements in coastal sediments of Iran's main oil terminal (Khark Island). Environ. Pollut. 220, 720–731. https://doi.org/10.1016/j.envpol.2016.10.038.

Akindele, E.O., Omisakin, O.D., Oni, O.A., Aliu, O.O., Omoniyi, G.E., Akinpelu, O.T., 2020. Heavy metal toxicity in the water column and benthic sediments of a degraded tropical stream. Ecotoxicol. Environ. Saf. 190, 110153. https://doi.org/10.1016/j.ecoenv.2019.110153.

Alqurashi, A.F., Kumar, L., 2019. An assessment of the impact of urbanization and land use changes in the fast-growing cities of Saudi Arabia. Geocarto Int. 34, 78–97. https://doi.org/10.1080/10106049.2017.1367423.

ASTDR, 2005. Public health statement nickel. Public Heal. Serv. Agency Toxic Subst. Dis. Regist.

ATSDR, 2008. Chromium (Cr) Toxicity, Case Studies in Environmental Medicine: Chromium Toxicity.

Bancon-Montigny, C., Gonzalez, C., Delpoux, S., Avenzac, M., Spinelli, S., Mhadhbi, T., Mejri, K., Hlaili, A.S., Pringault, O., 2019. Seasonal changes of chemical contamination in coastal waters during sediment resuspension. Chemosphere 235, 651–661. https://doi.org/10.1016/j.chemosphere.2019.06.213.

Barandovski, L., Frontasyeva, M.V., Stafilov, T., Šajn, R., Ostrovnaya, T.M., 2015. Multi-element atmospheric deposition in Macedonia studied by the moss biomonitoring technique. Environ. Sci. Pollut. Res. 22, 16077–16097. https://doi.org/10.1007/s11356-015-4787-x.

Basta, N.T., Ryan, J.A., Chaney, R.L., 2005. Trace element chemistry in residual-treated Soil : key concepts and metal bioavailability. J. Environ. Qual. 34, 49–63.

Battista, G., de Lieto Vollaro, R., 2017. Correlation between air pollution and weather data in urban areas: assessment of the city of Rome (Italy) as spatially and temporally independent regarding pollutants. Atmos. Environ. 165, 240–247. https://doi.org/10.1016/j.atmosenv.2017.06.050.

Benson, N.U., Adedapo, A.E., Fred-Ahmadu, O.H., Williams, A.B., Udosen, E.D., Ayejuyo, O.O., Olajire, A.A., 2018. A new method for assessment of sediment-associated contamination risks using multivariate statistical approach. Methods (Orlando) 5, 268–276. https://doi.org/10.1016/j.mex.2018.03.005.

Bhattacharjee, S., Ghosh, S.K., Chen, J., 2019. Spatial interpolation. Stud. Comput. Intell. 839, 19–41. https://doi.org/10.1007/978-981-13-8664-0_2.

Biswas, H., Melesse, A.M., 2016. Regional Scale Groundwater Flow Modeling for Wakel River Basin: A Case Study of Southern Rajasthan. Springer Geography. https://doi.org/10.1007/978-3-319-18787-7_19.

Blake, S., Henry, T., Murray, J., Flood, R., Muller, M.R., Jones, A.G., Rath, V., 2016. Compositional multivariate statistical analysis of thermal groundwater provenance: a hydrogeochemical case study from Ireland. Appl. Geochem. 75, 171–188. https://doi.org/10.1016/j.apgeochem.2016.05.008.

Bluskov, S., Arocena, J.M., Omotoso, O.O., Young, J.P., 2005. Uptake, distribution, and speciation of chromium in *Brassica juncea*. Int. J. Phytoremediation 7, 153–165. https://doi.org/10.1080/16226510590950441.

Brady, J.P., Ayoko, G.A., Martens, W.N., Goonetilleke, A., 2014a. Enrichment, distribution and sources of heavy metals in the sediments of Deception Bay, Queensland, Australia. Mar. Pollut. Bull. 81, 248–255. https://doi.org/10.1016/j.marpolbul.2014.01.031.

Brady, J.P., Ayoko, G.A., Martens, W.N., Goonetilleke, A., 2014b. Temporal trends and bioavailability assessment of heavy metals in the sediments of Deception Bay, Queensland, Australia. Mar. Pollut. Bull. 89, 464–472. https://doi.org/10.1016/j.marpolbul.2014.09.030.

Caballero-Gallardo, K., Alcala-Orozco, M., Barraza-Quiroz, D., De la Rosa, J., Olivero-Verbel, J., 2020. Environmental risks associated with trace elements in sediments from Cartagena Bay, an industrialized site at the Caribbean. Chemosphere 242, 125173. https://doi.org/10.1016/j.chemosphere.2019.125173.

Celis-Hernandez, O., Rosales-Hoz, L., Cundy, A.B., Carranza-Edwards, A., Croudace, I.W., Hernandez-Hernandez, H., 2018. Historical trace element accumulation in marine sediments from the Tamaulipas shelf, Gulf of Mexico: an assessment of natural vs anthropogenic inputs. Sci. Total Environ. 622– 623, 325–336. https://doi.org/10.1016/j.scitotenv.2017.11.228.

Chen, M., Gan, Z., Qu, B., Chen, S., Dai, Y., Bao, X., 2019. Temporal and seasonal variation and ecological risk evaluation of flame retardants in seawater and sediments from Bohai Bay near Tianjin, China during 2014 to 2017. Mar. Pollut. Bull. 146, 874–883. https://doi.org/10.1016/j.marpolbul.2019.07.049.

De Vivo, B., Belkin, H.E., Lima, A., 2017. Environmental Geochemistry : Site Characterization, Data Analysis and Case Histories. Elsevier.

Del Tánago, M.G., De Jalón, D.G., 2006. Attributes for assessing the environmental quality of riparian zones. Limnética 25, 389–402.

DeVore, R.M., Butler, M.J., Wallace, M.C., Liley, S.L., Mertz, A.A., Sesnie, S.E., Gipson, P.S., 2016. Elk resource selection patterns in a semiarid riparian corridor. J. Wildl. Manag. 80, 479–489. https://doi.org/10.1002/jwmg.1040.

Douay, F., Pelfrêne, A., Planque, J., Fourrier, H., Richard, A., Roussel, H., Girondelot, B., 2013. Assessment of potential health risk for inhabitants living near a former lead smelter. Part 1: metal concentrations in soils, agricultural crops, and homegrown vegetables. Environ. Monit. Assess. 185, 3665–3680. https://doi.org/10.1007/s10661-012-2818-3.

Duodu, G.O., Goonetilleke, A., Ayoko, G.A., 2016. Comparison of pollution indices for the assessment of heavy metal in Brisbane River sediment. Environ. Pollut. 219, 1077–1091. https://doi.org/10.1016/j.envpol.2016.09.008.

Egozcue, J.J., Pawlowsky-Glahn, V., Mateu-Figueras, G., Barceló-Vidal, C., 2003. Isometric logratio transformations for compositional data analysis. Math. Geol.

35, 279–300. https://doi.org/10.1023/A:1023818214614.
ELTurk, M., Abdullah, R., Rozainah, M.Z., Abu Bakar, N.K., 2018. Evaluation of heavy metals and environmental risk assessment in the Mangrove Forest of Kuala Selangor estuary, Malaysia. Mar. Pollut. Bull. 136, 1–9. https://doi.org/10.1016/j.marpolbul.2018.08.063.
Emenike, C.P., Okwuonu, E.J., Tenebe, I.T., Omole, D.O., Nwani, M., Afolayan, O.D., Oniemayin, B.I., 2019a. Ecological risk estimation of heavy metal pollution in roadside dust of Ado-Odo Ota, Southwestern Nigeria. IOP Conf. Ser. Mater. Sci. Eng. 640 https://doi.org/10.1088/1757-899X/640/1/012100.
Emenike, P.C., Nnaji, C.C., Tenebe, I.T., 2018. Assessment of geospatial and hydrochemical interactions of groundwater quality, southwestern Nigeria. Environ. Monit. Assess. 190 https://doi.org/10.1007/s10661-018-6799-8.
Emenike, P.C., Nnaji, C.C., Tenebe, I.T., Agunwamba, J.C., 2020a. Hydrogeochemical imprints and spatio-temporal health risk assessment of lead in drinking water sources of Abeokuta, south-western Nigeria. Int. J. Environ. Sci. Technol. 17, 343–360. https://doi.org/10.1007/s13762-019-02506-0.
Emenike, P.C., Neris, J.B., Tenebe, I.T., Nnaji, C.C., Jarvis, P., 2020b. Estimation of some trace metal pollutants in River Atuwara southwestern Nigeria and spatio-temporal human health risks assessment. Chemosphere 239. https://doi.org/10.1016/j.chemosphere.2019.124770.
Emenike, P.C., Tenebe, I., Ogarekpe, N., Omole, D., Nnaji, C., 2019b. Probabilistic risk assessment and spatial distribution of potentially toxic elements in groundwater sources in Southwestern Nigeria. Sci. Rep. 9, 1–15. https://doi.org/10.1038/s41598-019-52325-z.
Equeenuddin, S.M., Tripathy, S., Sahoo, P.K., Panigrahi, M.K., 2013. Metal behavior in sediment associated with acid mine drainage stream: role of pH. J. Geochem. Explor. 124, 230–237. https://doi.org/10.1016/j.gexplo.2012.10.010.
Ferguson, A.C., Black, J.C., Sims, I.B., Welday, J.N., Elmir, S.M., Goff, K.F., Higginbotham, J.M., Solo-Gabriele, H.M., 2018. Risk assessment for children exposed to arsenic on baseball fields with contaminated fill material. Int. J. Environ. Res. Publ. Health 15. https://doi.org/10.3390/ijerph15010067.
Fernandez-Maestre, R., Johnson-Restrepo, B., Olivero-Verbel, J., 2018. Heavy metals in sediments and fish in the caribbean coast of Colombia: assessing the environmental risk. Int. J. Environ. Res. 12, 289–301. https://doi.org/10.1007/s41742-018-0091-1.
Gaberšek, M., Gosar, M., 2018. Geochemistry of urban soil in the industrial town of Maribor, Slovenia. J. Geochem. Explor. 187, 141–154. https://doi.org/10.1016/j.gexplo.2017.06.001.
Gao, B., Gao, L., Xu, D., Zhou, Y., Lu, J., 2018. Assessment of Cr pollution in tributary sediment cores in the Three Gorges Reservoir combining geochemical baseline and in situ DGT. Sci. Total Environ. 628–629, 241–248. https://doi.org/10.1016/j.scitotenv.2018.01.322.
Gorny, J., Billon, G., Lesven, L., Dumoulin, D., Madé, B., Noiriel, C., 2015. Arsenic behavior in river sediments under redox gradient: a review. Sci. Total Environ. 505, 423–434. https://doi.org/10.1016/j.scitotenv.2014.10.011.
Guan, J., Wang, J., Pan, H., Yang, C., Qu, J., Lu, N., Yuan, X., 2018. Heavy metals in Yinma River sediment in a major Phaeozems zone, Northeast China: distribution, chemical fraction, contamination assessment and source apportionment. Sci. Rep. 8, 1–11. https://doi.org/10.1038/s41598-018-30197-z.
Güler, C., Kurt, M.A., Alpaslan, M., Akbulut, C., 2012. Assessment of the impact of anthropogenic activities on the groundwater hydrology and chemistry in Tarsus coastal plain (Mersin, SE Turkey) using fuzzy clustering, multivariate statistics and GIS techniques. J. Hydrol 414–415, 435–451. https://doi.org/10.1016/j.jhydrol.2011.11.021.
Hakanson, L., 1980. An ecological risk index for aquatic pollution control. A sedimentological approach. Water Res. 14, 975–1001.
He, Z., Li, F., Dominech, S., Wen, X., Yang, S., 2019. Heavy metals of surface sediments in the Changjiang (Yangtze River) Estuary: distribution, speciation and environmental risks. J. Geochem. Explor. 198, 18–28. https://doi.org/10.1016/j.gexplo.2018.12.015.
Hua, A.K., Ping, O.W., 2018. The influence of land-use/land-cover changes on land surface temperature: a case study of Kuala Lumpur metropolitan city. Eur. J. Remote Sens. 51, 1049–1069. https://doi.org/10.1080/22797254.2018.1542976.
IAEA, 2003. Collection and Preparation of Bottom Sediment Samples for Analysis of Radionuclides and Trace Elements. IAEA-TECDOC-1360.
ITRC, 2017. Bioavailability of Contaminants in Soil: Consideration for Human Health Risk Assessment [WWW Document]. Interstate Technol. Regul. Counc. Bioavailab. Contam. Soil Team. URL. accessed 11.23.19. https://bcs-1.itrcweb.org/9-1-risk-calculations/.
Keshavarzi, B., Hassanaghaei, M., Moore, F., Rastegari Mehr, M., Soltanian, S., Lahijanzadeh, A.R., Sorooshian, A., 2018. Heavy metal contamination and health risk assessment in three commercial fish species in the Persian Gulf. Mar. Pollut. Bull. 129, 245–252. https://doi.org/10.1016/j.marpolbul.2018.02.032.
Kozul-Wright, R., Fortunato, P., 2019. Development unchained: trade and industrialization in the era of international production. Glob. Policy 10, 29–40. https://doi.org/10.1111/1758-5899.12601.
Kusin, F.M., Azani, N.N.M., Hasan, S.N.M.S., Sulong, N.A., 2018. Distribution of heavy metals and metalloid in surface sediments of heavily-mined area for bauxite ore in Pengerang, Malaysia and associated risk assessment. Catena 165, 454–464. https://doi.org/10.1016/j.catena.2018.02.029.
Li, M., Zhang, Q., Sun, X., Karki, K., Zeng, C., Pandey, A., Rawat, B., Zhang, F., 2019. Heavy metals in surface sediments in the trans-Himalayan Koshi River catchment: distribution, source identification and pollution assessment. Chemosphere 244, 125410. https://doi.org/10.1016/j.chemosphere.2019.125410.
Liu, H., Xiong, Z., Jiang, X., Liu, G., Liu, W., 2016. Heavy metal concentrations in riparian soils along the Han River, China: the importance of soil properties, topography and upland land use. Ecol. Eng. 97, 545–552. https://doi.org/10.1016/j.ecoleng.2016.10.060.
Liu, S., Pan, G., Zhang, Y., Xu, J., Ma, R., Shen, Z., Dong, S., 2019. Risk assessment of soil heavy metals associated with land use variations in the riparian zones of a typical urban river gradient. Ecotoxicol. Environ. Saf. 181, 435–444. https://doi.org/10.1016/j.ecoenv.2019.04.060.
Liu, X., Zhang, L., Zhang, L., 2017. Concentration, risk assessment, and source identification of heavy metals in surface sediments in Yinghai: a shellfish cultivation zone in Jiaozhou Bay, China. Mar. Pollut. Bull. 121, 216–221. https://doi.org/10.1016/j.marpolbul.2017.05.063.
Maanan, Mohamed, Saddik, M., Maanan, Mehdi, Chaibi, M., Assobhei, O., Zourarah, B., 2015. Environmental and ecological risk assessment of heavy metals in sediments of Nador lagoon, Morocco. Ecol. Indicat. 48, 616–626. https://doi.org/10.1016/j.ecolind.2014.09.034.
MacDonald, D.D., Ingersoll, C.G., Berger, T.A., 2000. Development and evaluation of consensus-based sediment quality guidelines for freshwater ecosystems. Arch. Environ. Contam. Toxicol. 39, 20–31. https://doi.org/10.1007/s002440010075.
Madzin, Z., Shai-in, M.F., Kusin, F.M., 2015. Comparing heavy metal mobility in active and abandoned mining sites at bestari jaya, selangor. Procedia Environ. Sci. 30, 232–237. https://doi.org/10.1016/j.proenv.2015.10.042.
Mama, C.N., Nnaji, C.C., Emenike, P.C., Chibueze, C.V., 2020. Potential environmental and human health risk of soil and roadside dust in a rapidly growing urban settlement. Int. J. Environ. Sci. Technol. 17, 2385–2400. https://doi.org/10.1007/s13762-020-02637-9.
Mao, L., Liu, L., Yan, N., Li, F., Tao, H., Ye, H., Wen, H., 2020. Factors controlling the accumulation and ecological risk of trace metal(loid)s in river sediments in agricultural field. Chemosphere 243, 1–10. https://doi.org/10.1016/j.chemosphere.2019.125359.
McGrane, S.J., 2016. Impacts of urbanisation on hydrological and water quality dynamics, and urban water management: a review. Hydrol. Sci. J. 61, 2295–2311. https://doi.org/10.1080/02626667.2015.1128084.
Mukhopadhyay, S., Masto, R.E., Yadav, A., George, J., Ram, L.C., Shukla, S.P., 2016. Soil quality index for evaluation of reclaimed coal mine spoil. Sci. Total Environ. 542, 540–550. https://doi.org/10.1016/j.scitotenv.2015.10.035.
Müller, G., 1969. Index of geoaccumulation in sediments of the rhine river. Geol. J. 2, 108–118.
Naifar, I., Pereira, F., Zmemla, R., Bouaziz, M., Elleuch, B., Garcia, D., 2018. Spatial distribution and contamination assessment of heavy metals in marine sediments of the southern coast of Sfax, Gabes Gulf, Tunisia. Mar. Pollut. Bull. 131, 53–62. https://doi.org/10.1016/j.marpolbul.2018.03.048.
National Population Commission, 2010. Population Distribution by Sex,-State,LGA&Senatorial District, 2006 Population and Housing Census.
NCM, 2003. Cadmium review. Cadmium Rev 26.
NRC, 2003. Bioavailability of Contaminants in Soil and Sediment: Processes, Tools, and Applications. The National Academies Press, Washington, D.C.
Obiora, S.C., Chukwu, A., Davies, T.C., 2016. Heavy metals and health risk assessment of arable soils and food crops around Pb e Zn mining localities in Enyigba. southeastern Nigeria 116, 182–189. https://doi.org/10.1016/j.jafrearsci.2015.12.025.
Ogbiye, A.S., 2011. Pollution Problems and an Engineering Approach to the Management and Control of Industrial Effluents in Otta. Covenant University.
Omole, D.O., 2011. Evaluation of Water Quality Modelling Parameters : towards the Evolvement of Re-aeration Coefficient for Rivers in the Nigerian Environment. Covenant University.
Ouyang, W., Wang, Y., Lin, C., He, M., Hao, F., Liu, H., Zhu, W., 2018. Heavy metal loss from agricultural watershed to aquatic system: a scientometrics review. Sci. Total Environ. 208–220. https://doi.org/10.1016/j.scitotenv.2018.04.434, 637–638.
Oyeleran-Oyeyanka, O., 2015. Industrialization pathways to Hhuman development: industrial clusters, institutions and multidimensional poverty in Nigeria. In: Harnessing Africa's Growth for Faster Poverty Reduction, pp. 1–36.
Palansooriya, K.N., Shaheen, S.M., Chen, S.S., Tsang, D.C.W., Hashimoto, Y., Hou, D., Bolan, N.S., Rinklebe, J., Ok, Y.S., 2020. Soil amendments for immobilization of potentially toxic elements in contaminated soils: a critical review. Environ. Int. 134 https://doi.org/10.1016/j.envint.2019.105046.
Pandey, J., Singh, R., 2017. Heavy metals in sediments of Ganga River: up- and downstream urban influences. Appl. Water Sci. 7, 1669–1678. https://doi.org/10.1007/s13201-015-0334-7.
Patra, S., Sahoo, S., Mishra, P., Mahapatra, S.C., 2018. Impacts of urbanization on land use/cover changes and its probable implications on local climate and groundwater level. J. Urban Manag. 7, 70–84. https://doi.org/10.1016/j.jum.2018.04.006.
Pavlović, P., Mitrović, M., Dordević, D., Sakan, S., Slobodnik, J., Liška, I., Csanyi, B., Jarić, S., Kostić, O., Pavlović, D., Marinković, N., Tubić, B., Paunović, M., 2016. Assessment of the contamination of riparian soil and vegetation by trace metals - a Danube River case study. Sci. Total Environ. 540, 396–409. https://doi.org/10.1016/j.scitotenv.2015.06.125.
Pawlowsky-Glahn, V., Buccianti, A., 2011. Compositional Data Analysis: Theory and Applications, Compositional Data Analysis: Theory and Applications. https://doi.org/10.1002/9781119976462.
Petrik, A., Albanese, S., Lima, A., De Vivo, B., 2018a. The spatial pattern of beryllium and its possible origin using compositional data analysis on a high-density topsoil data set from the Campania Region (Italy). Appl. Geochem. 91, 162–173. https://doi.org/10.1016/j.apgeochem.2018.02.008.

Petrik, A., Thiombane, M., Albanese, S., Lima, A., De Vivo, B., 2018b. Source patterns of Zn, Pb, Cr and Ni potentially toxic elements (PTEs) through a compositional discrimination analysis: a case study on the Campanian topsoil data. Geoderma 331, 87–99. https://doi.org/10.1016/j.geoderma.2018.06.019.

Prieto, D.M., Martín-Liñares, V., Piñeiro, V., Barral, M.T., 2016. Arsenic transfer from as-rich sediments to river water in the presence of biofilms. J. Chem. 1–14. https://doi.org/10.1155/2016/6092047, 2016.

Pulles, T., Denier van der Gon, H., Appelman, W., Verheul, M., 2012. Emission factors for heavy metals from diesel and petrol used in European vehicles. Atmos. Environ. 61, 641–651. https://doi.org/10.1016/j.atmosenv.2012.07.022.

Ramião, J.P., Cássio, F., Pascoal, C., 2020. Riparian land use and stream habitat regulate water quality. Limnologica 82. https://doi.org/10.1016/j.limno.2020.125762.

Rasool, A., Farooqi, A., Masood, S., Hussain, K., 2016. Arsenic in groundwater and its health risk assessment in drinking water of Mailsi, Punjab, Pakistan. Hum. Ecol. Risk Assess. 22, 187–202. https://doi.org/10.1080/10807039.2015.1056295.

Reimann, C., Filzmoser, P., Garrett, R.G., 2002. Factor analysis applied to regional geochemical data: problems and possibilities. Appl. Geochem. 17, 185–206. https://doi.org/10.1016/S0883-2927(01)00066-X.

Rinklebe, J., Antoniadis, V., Shaheen, S.M., Rosche, O., Altermann, M., 2019. Health risk assessment of potentially toxic elements in soils along the Central Elbe River , Germany. Environ. Int. 126, 76–88. https://doi.org/10.1016/j.envint.2019.02.011.

Rodrik, D., 2016. Premature Deindustrialization. https://doi.org/10.12816/0022935.

Sakan, S.M., Dordević, D.S., Manojlović, D.D., Predrag, P.S., 2009. Assessment of heavy metal pollutants accumulation in the Tisza river sediments. J. Environ. Manag. 90, 3382–3390. https://doi.org/10.1016/j.jenvman.2009.05.013.

Saleem, M., Iqbal, J., Shah, M.H., 2015. Geochemical speciation, anthropogenic contamination, risk assessment and source identification of selected metals in freshwater sediments - a case study from Mangla Lake, Pakistan. Environ. Nanotechnol., Monit. Manag. 4, 27–36. https://doi.org/10.1016/j.enmm.2015.02.002.

Seshan, B.R.R., Natesan, U., Deepthi, K., 2010. Geochemical and statistical approach for evaluation of heavy metal pollution in core sediments in southeast coast of India. Int. J. Environ. Sci. Technol. 7, 291–306. https://doi.org/10.1007/BF03326139.

Shawul, A.A., Chakma, S., 2019. Spatiotemporal detection of land use/land cover change in the large basin using integrated approaches of remote sensing and GIS in the Upper Awash basin, Ethiopia. Environ. Earth Sci. 78, 1–13. https://doi.org/10.1007/s12665-019-8154-y.

Shen, F., Liao, R., Ali, A., Mahar, A., Guo, D., Li, R., Sun, X., Awasthi, M.K., Wang, Q., Zhang, Z., 2017. Spatial distribution and risk assessment of heavy metals in soil near a Pb/Zn smelter in Feng County, China. Ecotoxicol. Environ. Saf. 139, 254–262. https://doi.org/10.1016/j.ecoenv.2017.01.044.

Souri, A., Niyogi, S., Naji, A., 2019. Distribution , Source Apportionment , Bioavailability and Ecological Risks of Metals in Reef Sediments and Corals of the Persian Gulf (Iran): Khark Island , Chirouyeh , and Hendorabi Island 149. https://doi.org/10.1016/j.marpolbul.2019.110654.

Sucharovà, J., Suchara, I., Hola, M., Marikova, S., Reimann, C., Boyd, R., Filzmoser, P., Englmaier, P., 2012. Top-/bottom-soil ratios and enrichment factors: what do they really show? Appl. Geochem. 27, 138–145. https://doi.org/10.1016/j.apgeochem.2011.09.025.

Sun, C., Zhang, Z., Cao, H., Xu, M., Xu, L., 2019. Concentrations, speciation, and ecological risk of heavy metals in the sediment of the Songhua River in an urban area with petrochemical industries. Chemosphere 219, 538–545. https://doi.org/10.1016/j.chemosphere.2018.12.040.

Tenebe, I.T., Emenike, C.P.G., Daniel Chukwuka, C., 2018. Prevalence of heavy metals and computation of its associated risk in surface water consumed in Ado-Odo Ota, South-West Nigeria. Hum. Ecol. Risk Assess. 1–23. https://doi.org/10.1080/10807039.2018.1454824, 0.

Thiombane, M., Martín-Fernández, J.A., Albanese, S., Lima, A., Doherty, A., De Vivo, B., 2018. Exploratory analysis of multi-element geochemical patterns in soil from the Sarno River Basin (Campania region, southern Italy) through compositional data analysis (CODA). J. Geochem. Explor. 195, 110–120. https://doi.org/10.1016/j.gexplo.2018.03.010.

Tolosana-Delgado, R., McKinley, J., 2016. Exploring the joint compositional variability of major components and trace elements in the Tellus soil geochemistry survey (Northern Ireland). Appl. Geochem. 75, 263–276. https://doi.org/10.1016/j.apgeochem.2016.05.004.

UNIDO, 2018. Demand for Manufacturing: Driving Inclusive and Sustainable Industrial Development. https://doi.org/10.18356/62a26775-en.

US EPA, 2012. Recommendations for Default Value for Relative Bioavailability of Arsenic in Soil [WWW Document]. OSWER 9200.1-113. Washington, D.C. URL. https://www.epa.gov/superfund/soil-bioavailability-superfund-sites-guidance#arsenic.

US EPA, 2005. Environmental Protection Agency. Guidelines for Carcinogen Risk Assessment.

US EPA, 1989. Risk Assessment Guidance for Superfund Volume I Human Health Evaluation Manual (Part A). US EPA. EPA/540/1-89/002.

van den Boogaart, K.G., Tolosana-Delgado, R., 2013. Analyzing compositional data with R. Anal. Compos. Data with R 1–258. https://doi.org/10.1007/978-3-642-36809-7.

Wang, A.T., Wang, Q., Li, J., Yuan, G.L., Albanese, S., Petrik, A., 2019. Geo-statistical and multivariate analyses of potentially toxic elements' distribution in the soil of Hainan Island (China): a comparison between the topsoil and subsoil at a regional scale. J. Geochem. Explor. 197, 48–59. https://doi.org/10.1016/j.gexplo.2018.11.008.

Wang, S., Mulligan, C.N., 2006. Effect of natural organic matter on arsenic release from soils and sediments into groundwater. Environ. Geochem. Health 28, 197–214. https://doi.org/10.1007/s10653-005-9032-y.

Weissmannová, H.D., Pavlovský, J., 2017. Indices of soil contamination by heavy metals – methodology of calculation for pollution assessment (minireview). Environ. Monit. Assess. 189 https://doi.org/10.1007/s10661-017-6340-5.

Wu, S., Peng, S., Zhang, X., Wu, D., Luo, W., Zhang, T., et al., 2015. Levels and health risk assessments of heavy metals in urban soils in Dongguan, China. J. Geochem. Explor. 148, 71–78. https://doi.org/10.1016/j.gexplo.2014.08.009.

Wuana, R.A., Okieimen, F.E., 2011. Heavy metals in contaminated soils: a review of sources, chemistry, risks and best available strategies for remediation. ISRN Ecol 1–20. https://doi.org/10.5402/2011/402647, 2011.

Xiang, H., Zhang, Y., Richardson, J.S., 2016. Importance of riparian zone: effects of resource availability at land-water interface. Riparian Ecol. Conserv. 3, 1–17. https://doi.org/10.1515/remc-2016-0001.

Xu, L., Zhao, Z., Wang, S., Pan, R., Jia, Y., 2011. Transformation of arsenic in offshore sediment under the impact of anaerobic microbial activities. Water Res. 45, 6781–6788. https://doi.org/10.1016/j.watres.2011.10.041.

Zahra, A., Hashmi, M.Z., Malik, R.N., Ahmed, Z., 2014. Enrichment and geo-accumulation of heavy metals and risk assessment of sediments of the Kurang Nallah-Feeding tributary of the Rawal Lake Reservoir, Pakistan. Sci. Total Environ. 470–471, 925–933. https://doi.org/10.1016/j.scitotenv.2013.10.017.

Zha, Y., Gao, J., Ni, S., 2003. Use of normalized difference built-up index in automatically mapping urban areas from TM imagery. Int. J. Rem. Sens. 24, 583–594. https://doi.org/10.1080/01431160304987.

Zhang, G., Bai, J., Zhao, Q., Lu, Q., Jia, J., Wen, X., 2016. Heavy metals in wetland soils along a wetland-forming chronosequence in the Yellow River Delta of China : levels , sources and toxic risks. Ecol. Indicat. 69, 331–339. https://doi.org/10.1016/j.ecolind.2016.04.042.

Zhang, Z.W., Xu, X.R., Sun, Y.X., Yu, S., Chen, Y.S., Peng, J.X., 2014. Heavy metal and organic contaminants in mangrove ecosystems of China: a review. Environ. Sci. Pollut. Res. 21, 11938–11950. https://doi.org/10.1007/s11356-014-3100-8.

Zhu, Z., Sun, G., Bi, X., Li, Z., Yu, G., 2013. Identification of trace metal pollution in urban dust from kindergartens using magnetic, geochemical and lead isotopic analyses. Atmos. Environ. 77, 9–15. https://doi.org/10.1016/j.atmosenv.2013.04.053.

Zhuang, Q., Li, G., Liu, Z., 2018. Distribution, source and pollution level of heavy metals in river sediments from South China. Catena 170, 386–396. https://doi.org/10.1016/j.catena.2018.06.037.

Zuzolo, D., Cicchella, D., Catani, V., Giaccio, L., Guagliardi, I., Esposito, L., De Vivo, B., 2017. Assessment of potentially harmful elements pollution in the Calore River basin (Southern Italy). Environ. Geochem. Health 39, 531–548. https://doi.org/10.1007/s10653-016-9832-2.